Adv Polym Sci (2013) 251: 77–140
DOI: 10.1007/12_2012_167

Published online: 18 March 2012

Recent Advances in High-Temperature Fractionation of Polyolefins

Harald Pasch, Muhammad Imran Malik, and Tibor Macko

Abstract The synthesis and characterization of polyolefins continues to be one of the most important areas for academic and industrial research. One consequence of the development of new "tailor-made" polyolefins is the need for new and improved analytical techniques for the analysis of polyolefins with respect to molar mass, molecular topology and chemical composition distribution. This review presents different new and relevant techniques for polyolefin analysis. The analysis of copolymers by combining high-temperature SEC and FTIR spectroscopy yields information on chemical composition and molecular topology as a function of molar mass. Crystallization based fractionation techniques are powerful methods for the analysis of short-chain branching in LLDPE and the analysis of polyolefin blends. These methods include temperature-rising elution fractionation, crystallization analysis fractionation and the recently developed crystallization-elution fractionation.

The latest development in the field of polyolefin fractionation is high-temperature interaction chromatography. Based on the principles of gradient HPLC and liquid chromatography at critical conditions this method is used for fast analysis of the chemical composition distribution of complex olefin copolymers. The efficiency of HPLC based systems for the separation of various olefin copolymers will be discussed. The ultimate development in high-temperature fractionation of polyolefins is comprehensive high-temperature two-dimensional liquid chromatography. The review will discuss some of the pioneering work that has been done since 2008.

H. Pasch (✉)
Department of Chemistry and Polymer Science, University of Stellenbosch, Private Bag X1, 7602 Stellenbosch, South Africa
e-mail: hpasch@sun.ac.za

M.I. Malik
H.E.J. Research Institute of Chemistry, International Center for Chemical and Biological Sciences (ICCBS), University of Karachi, Karachi, Pakistan

T. Macko
German Institute for Polymers, Schlossgartenstr. 6, 64289 Darmstadt, Germany

Finally, the correlation between molar mass and chemical composition can be accessed by on-line coupling of high-temperature SEC and ^{1}H-NMR spectroscopy. It is shown that the on-line NMR analysis of chromatographic fractions from high-temperature fractionations is possible and yields information on microstructure and tacticity in addition to molar mass and copolymer composition.

Keywords Crystallization analysis fractionation · Field Flow Fractionation · High performance liquid chromatography · Hyphenated techniques · Liquid chromatography · Polyolefin analysis · SEC-NMR coupling · Size exclusion chromatography · Temperature rising elution fractionation · Two-dimensional liquid chromatography

Contents

Abbreviations

AFFFF, AF4	Asymmetric flow field flow fractionation
A-TREF	Analytical temperature rising elution fractionation
CCD	Chemical composition distribution
CEF	Crystallization elution fractionation
CRYSTAF	Crystallization analysis fractionation
2D-LC	Two-dimensional liquid chromatography
DSC	Differential scanning calorimetry
EGMBE	Ethylene glycol monobutylether
ELSD	Evaporative light scattering detector
EPDM	Ethylene-propylene-diene monomer
EVA	Ethylene-vinyl acetate
FFF	Field flow fractionation
FTIR	Fourier transform infrared
HDPE	High density polyethylene
HPLC	High performance liquid chromatography
HT	High temperature
IC	Interactive chromatography

ICPP	Impact polypropylene copolymer
IR	Infrared
LAM	Longitudinal acoustic mode
LCCC	Liquid chromatography at critical conditions
LDPE	Low-density polyethylene
LLDPE	Linear low-density polyethylene
MALLS	Multi angle laser light scattering
MALS	Multi angle light scattering
MMA	Methylmethacrylate
MT-AF4	Medium temperature asymmetric flow field flow fractionation
M_n	Number average molar mass
M_w	Weight average molar mass
MM	Molar mass
MMD	Molar mass distribution
NMR	Nuclear magnetic resonance
ODCB	1,2-Dichlorobenzene
PBA	Polybutylacrylate
PE	Polyethylene
PMMA	Polymethylmethacrylate
PP	Polypropylene
PS-DVB	Polystyrene-divinylbenzene copolymer
P-TREF	Preparative temperature rising elution fractionation
PVAc	Polyvinylacetate
RALLS	Right angle laser light scattering
R_g	Radius of gyration
RI	Refractive index
SEC	Size exclusion chromatography
SEM	Scanning electron microscopy
SSA	Successive self-nucleation annealing
SSF	Successive solution fractionation
TCB	1,2,4-Trichlorobenzene
TGA	Thermo-gravimetric analysis
TGIC	Temperature gradient interactive chromatography
TREF	Temperature rising elution fractionation
UHM	Ultra high molar mass
VA	Vinyl acetate
VIS	Viscosimetric detector
WAXD	Wide angle X-ray diffraction

1 Introduction

The polymerization of olefins to polymers with different microstructures and properties continues to be one of the most investigated areas for both industrial and academic laboratories in polymer science. The use of polyolefins as polymeric

materials is rapidly growing due to the fact that polyolefins are made from simple and easily available monomers. In addition, they contain only carbon and hydrogen, and can be reused or degraded by thermal processes to oil and monomers [1]. New or improved properties are achieved by combining new monomers in a copolymer system, or by using new catalysts. Forty years after the discovery of the metallorganic catalyzed polymerization of olefins by Ziegler and the stereospecific polymerization of propene and α-olefins by Natta [2], the use of metallocene catalysts [3] shows the way to expand the possibilities of olefin polymerization and the properties of the resulting polyolefin materials. Polyolefins are the most widely used synthetic polymers, their annual production exceeding 100 million metric tons. Polyolefin production continues to grow exponentially [4].

One consequence of the development of new "tailor-made" polyolefins is the need for new and improved analytical techniques. In addition to monitoring the polymerization process, the molecular heterogeneity of the resulting products must be described by suitable methods. Irrespective of whether a Ziegler–Natta or a metallocene catalyst is used, information on molar mass distribution (MMD), chemical composition, tacticity, and molecular topology (branching) is required to evaluate properly a polymeric material. Very frequently, polyolefins exhibit multiple distributions, e.g., long chain branching and MMD in low-density polyethylene (LDPE) or chemical composition distribution (CCD) and MMD in linear low-density polyethylene (LLDPE), copolymers and polymer blends.

The present article reviews different relevant techniques for polyolefin fractionation. A number of important methods are well established that provide average information on the molecular structure of polyolefins, the most prominent ones being FTIR and NMR spectroscopy for the average chemical composition and microstructure, viscometry, and light scattering for the average molar mass, and thermal analysis for glass transition, melting and crystallization temperatures and enthalpies. These averaging techniques do not provide information on the distributions in chemical composition and molar mass which are most important parameters for structure–property correlations. Distributions in molecular parameters can only be obtained by suitable fractionation methods.

Most polymer fractionation methods work in dilute polymer solutions requiring proper solubility of all polymer components in the solvent that is used for the fractionation procedure. The majority of technically important polyolefins are semicrystalline materials with melting points above 100°C. They are not soluble in most of the typical organic solvents. Such stability against solvents is useful for practical applications; it is, however, a problem for solution based analytical methods. Typically, the polyolefin material must be heated above its melting temperature to be soluble and, therefore, specific high boiling point solvents are required in polyolefin analysis. A second problem is the fact that polyolefins tend to undergo thermo-oxidative degradation. This of course has to be prevented by suitable measures when dissolving the sample. Typically, polyolefins are dissolved at temperatures between 130 and 160°C. To prevent degradation, stabilizers and antioxidants are added to the solvent. The most common solvents for polyolefin fractionations are 1,2,4-trichlorobenzene (TCB), 1,2-dichlorobenzene, decaline, and in some cases cyclohexane [5, 6].

2 Crystallization Based Fractionation Techniques

These are a group of techniques based on the different crystallization behaviour of semicrystalline polyolefins in dilute solution to get information about CCD. The crystallization behaviour of polyolefins is determined by the molecular structure including the type of monomer, the copolymer composition and the molecular size. The crystallization behaviour as will be discussed in this section is dominated by the type of monomer and the copolymer composition.

The principles of polymer fractionation by solubility or crystallizability are based on the Flory–Huggins statistical thermodynamic treatment that accounts for melting-point depression by the presence of a diluent, and can be expressed as follows [7, 8]:

$$1/T_{\mathrm{m}} - 1/T_{\mathrm{m}}^{\mathrm{o}} = (R/\Delta H_{\mathrm{u}}) \ln N_{\mathrm{A}} \tag{1}$$

where $T_{\mathrm{m}}^{\mathrm{o}}$ is the melting temperature of the pure polymer, T_{m} is the equilibrium melting temperature of the "diluted" polymer, ΔH_{u} is the heat of fusion per polymer repeating unit, and N_{A} is the mole fraction of the diluent. A solvent or a comonomer can act as the diluent. In both cases the crystallization temperature decreases with increasing diluent concentration. Therefore, for copolymers the separation by crystallizability can be regarded as a separation by chemical composition.

In 1950, Desreux and Spiegels [9] recognized the potential of crystallization behaviour of semicrystalline polymers as an analytical tool. The major techniques in this category are temperature rising elution fractionation (TREF), crystallization analysis fractionation (CRYSTAF) and crystallization elution fractionation (CEF). All these techniques differentiate different polyolefins by differences in their crystallizability as a function of temperature but different experimental approaches are used to get the final results which will be discussed in detail as follows. The main disadvantage of crystallization based techniques is very long analysis time and research is mainly focused on decreasing analysis times along with other aspects like better resolution of different fractions. Another disadvantage is the fact that only the crystallizable part of a material can be fractionated. The amorphous part is obtained as a bulk fraction. In the early days of TREF, the analysis time was around 100 h per sample. Recent improvements in TREF allow analysis of a sample in 3–4 h while the development of CRYSTAF reduced this analysis time to 100 min. The latest development in crystallization based techniques – CEF – allows analyzing a sample in 30 min.

2.1 Temperature Rising Elution Fractionation

The term TREF was first used by Shirayama [10]. They fractionated low-density polyethylene (LDPE) according to the degree of chain branching. TREF can be performed on preparative (P-TREF) and analytical scale (A-TREF). These different

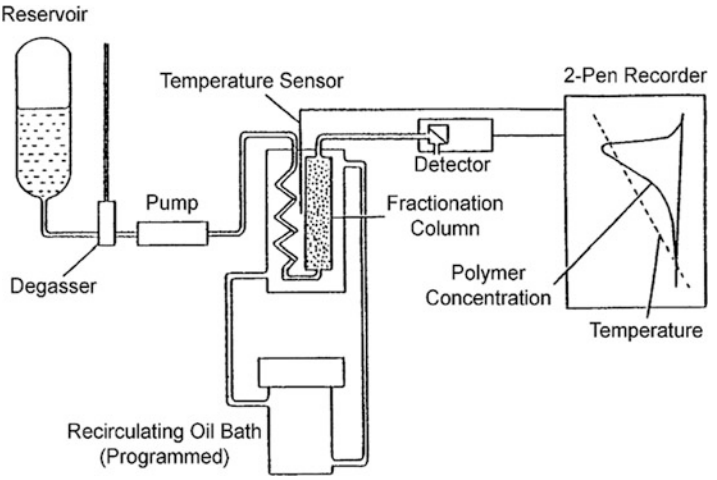

Fig. 1 Schematic diagram of analytical TREF. (Reprinted from [11] with permission of Springer Science + Business Media)

modes of TREF vary basically in the elution step and sample size. The apparatus for the analytical mode of TREF is shown schematically in Fig. 1.

Briefly, the polymer sample is first dissolved in a good solvent at high temperature. This solution is then introduced into a column filled with an inert carrier substance like glass beads or sea sand. The temperature is then decreased at a programmed slow and constant cooling rate (CR). This allows polymer chains to crystallize in orderly fashion from higher to lower crystallinities. The cooling rate is one of the key factors for the efficient separation of different fractions as the crystallization step mainly determines the quality of fractionation. In the second step pure solvent is passed through the column and the temperature is increased in a slow programmed manner.

In P-TREF, larger sample sizes and fractionation columns are used and the temperature is increased in steps. All polymer material eluting at a particular temperature interval is collected for further analysis by other techniques, e.g., size exclusion chromatography (SEC) or successive solution fractionation (SSF), FTIR or NMR.

In A-TREF, the column temperature is increased continuously and the polymer concentration in the eluent is measured with an online detector to obtain TREF profiles of weight fraction of eluted polymer vs. temperature. The temperature axis is subsequently translated into a chemical composition axis using a suitable calibration curve. The calibration curve of chemical composition (copolymer) vs. temperature is generated for particular experimental conditions (cooling rate, comonomer type, solvent, etc.) by using copolymer standards with narrow CCDs. These narrow CCD copolymers are typically obtained from P-TREF fractionation or direct synthesis using single-site catalysts. It has to be pointed out here that the

comonomer sequence distribution may affect the TREF and CRYSTAF calibration curves and must be taken into account.

There are several factors which can affect TREF profiles and the reliability of TREF results, namely the molar mass of the polymer, the comonomer type and content, the cooling rate, co-crystallization effects, etc. In the literature there are a number of reviews on TREF analysis, and some of the most important ones are given in [11–13]. The latest summary was given by Soares et al. [13] in 2005. In the present review we focus on developments in techniques and applications that appeared after 2005.

Tomba et al. [14] investigated the TREF fractionation process in detail. They showed by analysis of TREF fractions using Raman spectroscopy in longitudinal acoustic mode (LAM) and DSC that in CRYSTAF and TREF the slow crystallization of polyethylene occurs in the extended chain mode only at molar masses less than 2,000 g/mol. At higher molar masses with the same experimental conditions, chain folding takes place. In the case of polyolefin blends, independent crystallization was observed only for a narrow molar mass range while for broad molar mass ranges co-crystallization occurred. These results show that the unexpected crystallizable sequences which the same group reported earlier really exist and can be attributed to chain folding and co-crystallization phenomena. The Raman technique in LAM mode was the right tool for direct examination of the distribution of crystallizable sequence lengths. DSC could be used only when narrow distributions of crystallizable sequences were expected. Overall, these results show that the combination of a thermodynamic model and the inverse technique calculation procedure proposed by them give correct results for the calculation of distributions of lengths of crystallizable sequences from TREF fractograms.

The effect of the tacticity distribution on the thermo-oxidative degradation behaviour of polypropylene was investigated by Suzuki et al. [15]. NMR, TREF and TGA were used for this study. In order to investigate the effect of the tacticity distribution on degradation, TREF fractions were collected and subjected to TGA. The results indicate that the rate of degradation of polypropylene depended systematically on the tacticity distribution, suggesting that the higher stability of atactic PP originates from the hindered abstraction reaction of the tertiary hydrogen, which is the rate-determining step in PP degradation. Therefore it is concluded by them that the rate of thermo-oxidative degradation will increase systematically with the increase of meso sequences in the chain. Kissin et al. [16] developed a new approach for the detailed TREF analysis of ethylene/α-olefin copolymers prepared with multi-centre heterogeneous Ziegler–Natta catalysts. Their approach was based on the deconvolution of complex TREF curves into elemental components described with a Lorentz distribution function. Previous work by Soares and others was based on deconvolution of Stockmayer distributions. This approach was applied to a series of ethylene/1-butene copolymers prepared with a supported Ti based catalyst at different reaction times. It has been shown that copolymers with an average composition of 6.5–3.5 mol% of 1-butene actually consist of many discrete compositions ranging from 15 to 20 mol% of 1-butene to less than 1% of 1-butene. The comparison of TREF and SEC data provides complementary

information on the properties and nature of the active centres in the catalysts and their ability to copolymerize the α-olefin with ethylene. The molecular structure modelling for LDPE was proposed by Schmidt et al. [17]. Their simulation predictions were correlated with TREF-SEC analysis for actual microscopic structure of the material and by a reversed procedure entailing the correlation of the reaction conditions with the product properties. Of course, this is only an initial study in this context and more detailed studies for the refinement of the model are still needed.

Gupta et al. [18] developed structure–property relationships for linear low-density polyolefins with the same content of SCB but different lengths of the short chains (different comonomers were used including butene, hexene, octene). They correlated the mechanical properties of LLDPE with TREF data and found that products with similar TREF profiles may differ significantly in the mechanical properties of their films depending systematically on the type of comonomer used. In a study by Hasan et al. [19] Ziegler–Natta catalysts preparation procedures, the type of co-catalyst, the pre-treatment of the catalyst and the polymerization conditions were correlated with the resulting polypropylene tacticity. Data on molecular structure were obtained by SEC, NMR and TREF. The authors demonstrated that the type of the aluminium alkyl co-catalyst played the most dominant role for the isospecificity of the activated catalyst sites and their distribution. In addition to the type of co-catalyst, only the grinding method of the catalyst showed significant effects on the isospecific nature of active sites. Zhang and co-workers [20] studied random copolymers of propylene and ethylene containing 5.1 mol% ethylene by preparative TREF fractionation and subsequent analysis by SEC, ^{13}C NMR, differential scanning calorimetry, and wide-angle X-ray diffraction analysis. The results showed that the TREF fractions contained copolymer molecules with different compositions and molar masses. The isotacticity of the fractions increased with increasing elution temperature. Structure–property relationships were developed and it was shown that both the copolymer composition and the sequence distribution in the copolymer had significant effects on the thermal and crystallization behaviour. Fan and co-workers [21] studied compositional distributions of different particles of a polypropylene/poly (ethylene-*co*-propylene) blend by TREF. Their results from TREF and the ^{13}C-NMR analysis of TREF fractions showed that the composition distributions of the large and small particles were different. The large particles were rich in propylene homopolymer and ethylene/propylene block copolymer, whereas the small particles contained more ethylene/propylene random copolymer and copolymer with a transition microstructure. The fragmentation of the polymer particles may take place in the first (homopolymerization) and the second (copolymerization) steps. It is well known that particles of PP homopolymer are well fragmented, proving that a copolymerization step is not strictly required for particle fragmentation.

Zhang [22] reported on the systematic investigation of random copolymers of propylene with small amounts of 1-butene synthesized with a Ziegler–Natta catalyst to understand their molecular microstructure and crystallization behaviour. Fractions from TREF were analyzed by CRYSTAF, SEC and ^{13}C NMR. The results showed that the TREF fractions had relatively uniform microstructures with long isotactic

propylene sequences and the 1-butene comonomer as isolated units. Fractions at higher elution temperature contained less 1-butene. Melting temperatures decreased with increasing 1-butene content in the copolymers. Aust et al. [23] proposed an experimental design plan for optimization of the TREF process taking ethylene/propylene copolymers (EPC) as an example. It was shown that the separation quality can be remarkably improved by the aid of factoral design experiments. Starting at higher temperatures of crystallization had a strong positive impact while increases in cooling or heating rates affected the quality of separation negatively. They also asserted that knowledge of full experimental parameters is necessary to compare TREF results from different sources. Kissin and co-workers [24] used analytical TREF to study the distribution of isospecific centres in supported titanium based Ziegler–Natta catalysts (five catalyst systems were investigated). The number of TREF components and their relative amounts were substantially different for the crystalline fractions produced with different catalyst systems. The differences in catalyst behaviour were assigned to the nature of the internal and external electron donor capabilities of the catalysts. The conclusion of their study was that the probability of chain transfer reactions for different active centres decreases with the increase in the isospecificity of the centres. Van Reenen and co-workers [25] fractionated two commercial LLDPE (comonomers 1-butene and 1-hexene) with similar densities, MFI values and comonomer contents by TREF. They did further analysis of fractions by high resolution solution and solid state NMR. It was shown in this study that, although the amount of crystallinity was the same for both polymers, the type of crystallinity differed significantly. They argued that the hyphenation of TREF with NMR provided a wealth of information and insight into the microstructure of the polymers that was not possible otherwise. Harding and van Reenen [26] fractionated three propylene-ethylene random copolymers by using P-TREF and analyzed the fractions by CRYSTAF, DSC, ^{13}C NMR, HT-SEC and WAXD. It was shown by them that comonomer incorporation inhibits the crystallization of the copolymer and as the ethylene content increases, the crystallization and melting point decreases. They also depicted that an increased ethylene content leads to an increased formation of γ-phase crystals.

Terano and co-workers [27] reported two unique applications of TREF for polymerization kinetics of isospecific polypropylene and degradation behaviour of isotactic polypropylene. The $MgCl_2$ supported catalyst, triethylaluminium and toluene were stirred in a volumetric flask at 30°C for different time intervals and the catalyst was recovered by filtration. They noticed that the yield, the molar mass and the isotacticity of PP produced by catalysts after above extraction procedure, decrease with increasing treatment time by triethylaluminium, suggesting that the extraction of the internal donor critically affects the concentration of active sites in $TiCl_4/MgCl_2$ catalyst systems. The relationship between polymer tacticity and the degradation rate of isotactic polypropylene was also evaluated. Caballero et al. [28] synthesized and characterized copolymers of ethylene and propylene in the whole composition range using a supported metallocene based catalyst. They showed by their TREF and SEC-MALLS results that copolymers containing less than 10% and more than 80% of ethylene are semi-crystalline, having TREF elution temperatures

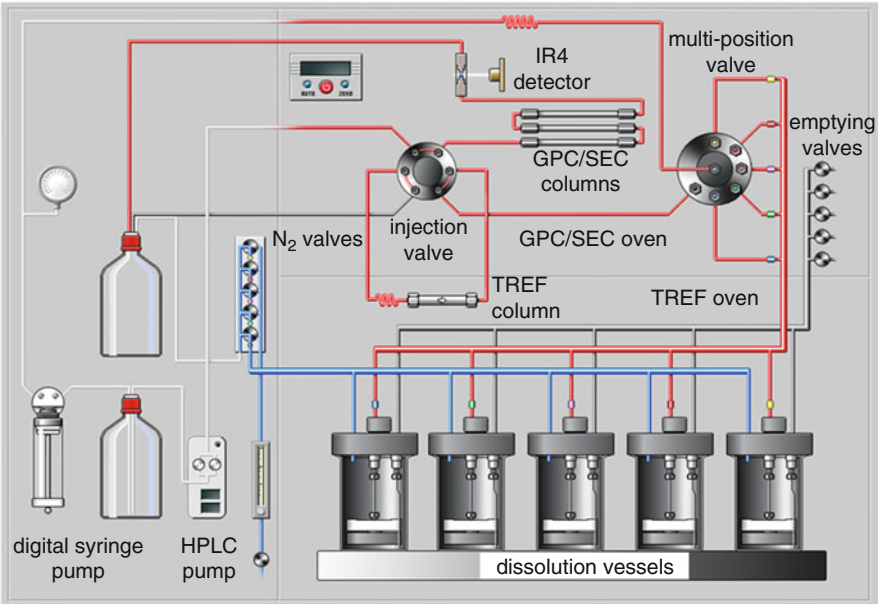

Fig. 2 Schematic diagram of an automated cross-fractionation instrument. Injection valve shown in "load" position A; "inject" position marked as B. (Reprinted from [30] with permission of Wiley-VCH)

typical for that kind of polymers. They also correlated the TREF results with final properties of the products.

Shan and Hazlitt [29] were successful in developing a "block index methodology" by collecting fractions from P-TREF and then subjecting them to A-TREF. They noticed that olefin block copolymer fractions eluting at the same TREF temperature have much higher comonomer contents than comparable fractions of random copolymers. Proper interpretation of their "block index" indicates the degree to which the intra-chain comonomer distribution is segmented or blocked. Monrabal and co-workers [30] developed an automated cross-fractionation apparatus (TREF-SEC), shown in Fig. 2, to characterize fully polyolefins with bivariate distributions. Several examples of applications have been presented like SCB distribution as a function of MMD of HDPE. They recommended the addition of other online detectors like methyl-sensitive IR sensors, viscometers and light scattering detectors for enhancing information.

The instrument was built by modifying the design of a TREF 300 unit (Polymer Char, Spain) which incorporates an oven used for sample preparation and a high precision TREF column oven. Other components are syringe pump, HPLC pump, high temperature isothermal oven (SEC oven) in which the injection valve, a multiposition selection valve and the SEC column set are placed. A dual band IR4 infrared detector (Polymer Char, Spain) is used as the concentration detector.

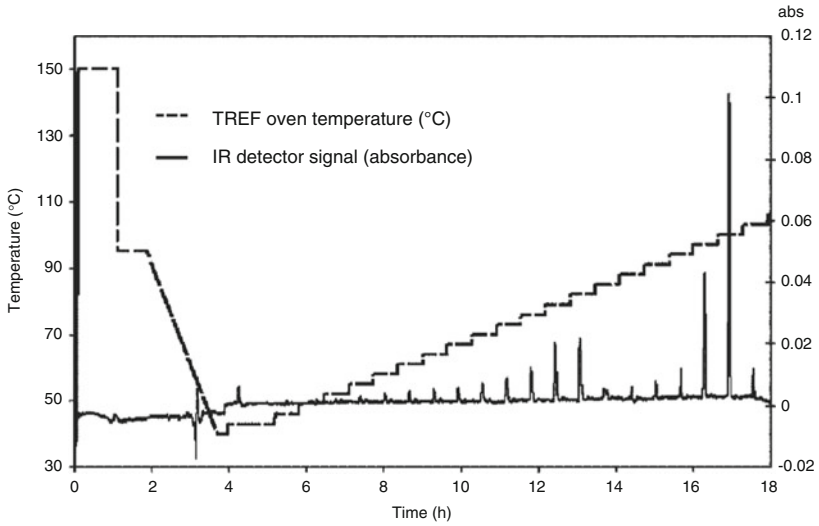

Fig. 3 IR detector signal and TREF oven temperature collected during a full cross-fractionation run. (Reprinted from [30] with permission of Wiley-VCH)

Inside the TREF oven a set of five stainless steel vessels with internal filters and magnetic stir bars is used for dissolution of up to five different samples that can be analyzed sequentially. Solvent is added to the vessels through a syringe pump, while the TREF oven is heated typically to 150°C. Once the polymer sample is fully dissolved, an aliquot is taken from the vessel through its internal filter and loaded into the TREF column by using the syringe pump again, moving the injection valve to the "load" position. Depending on the sample heterogeneity and number of fractions required, typically 1–3 mg of material are loaded into the TREF column. The polymer in the TREF column is then crystallized, typically at 0.5°C/min with no flow, keeping the injection valve in the "load" position during the crystallization process. Meanwhile, a stand-by flow of solvent is maintained through the SEC columns. The flow rate is increased, typically to 1.0 mL/min at a pre-defined stabilization time prior to the first injection. A typical temperature profile followed by the TREF oven along the full cross-fractionation analysis, where dissolution, crystallization, and stepwise elution are identified is shown in Fig. 3. Once the polymer has been crystallized and the fractions having different crystallinities have been segregated into the TREF column, a discontinuous elution process is followed at increasing temperature steps. At each temperature, and after a given dissolution time, the injection valve is switched to the "inject" position in order to allow the solvent to elute the dissolved polymer from the TREF column. Once that fraction is eluted, the injection valve is closed again to the "load" position so that the flow through the TREF column is stopped. Then, the oven temperature is increased to start dissolving the fraction that will be eluted in the next step. Following that process, different TREF fractions with increasing crystallinity are injected into the SEC columns,

where they are fractionated, this time according to molar mass. An IR4 infrared detector is used to record the final chromatograms continuously, as depicted in Fig. 3 where the raw IR detector and oven temperature signals from a real experiment are plotted. It must be noted that each of the peaks in the IR detector signal is in fact a full SEC chromatogram of one of the TREF fractions; therefore the MMD of each narrow-CCD fraction is obtained.

Information about microstructural distributions is one of the major goals of polyolefin analysis research. There are lots of mathematical models proposed that link polymerization kinetics to chain microstructure and polymer characterization results. Simple expressions can be used for polymers synthesized with single-site catalysts but these are not valid for multiple-site catalysts. Mathematical modelling for microstructural characterization has been reviewed by Soares and a few new mathematical expressions were derived that help to understand the results obtained with several polyolefin characterization techniques [31]. Ishihara et al. [32] studied various new malonates as internal donors for $MgCl_2$-supported $TiCl_4$ catalysts for propylene polymerization. From TREF results they concluded that the catalyst activity and the isotacticity of polypropylene depend not only on the oxygen electron density of the electron donor but also on the molecular volume of the internal donor. Yau [33] demonstrated the potential of a 3D-SEC-TREF hybrid system (see Fig. 4) for studying polyolefin microstructure and argued that automation of sample injection and temperature programming is the key for high precision analysis.

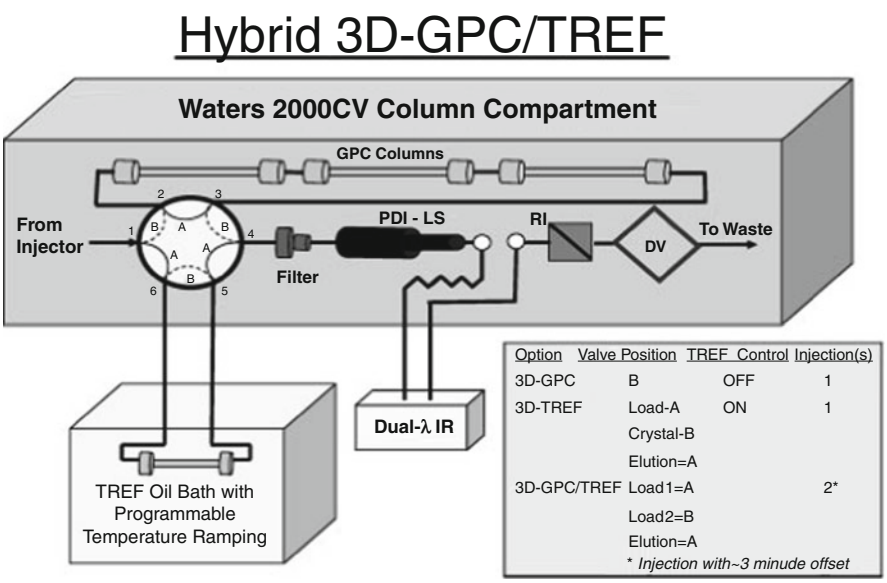

Fig. 4 Configuration of the hybrid 3D-SEC-TREF system. (Reprinted from [33] with permission of Wiley-VCH)

3D-SEC-TREF is not only useful in understanding microstructure but also in analyzing the composition of polymer blends and final products. Nakatani and co-workers [34] studied the thermo-oxidative degradation of impact polypropylene. They collected eight TREF fractions and studied them by ^{13}C NMR, FTIR and DSC. They found that the fractions were composed of homopolymers or blends of PP, PE and EPC. The content of tertiary C–H bonds and the existence of a 3_1 helix conformation corresponded to the PP crystalline part that dominates the rate of degradation. They pointed out that the systematic analysis of polyolefin degradation using TREF is a useful method to clarify the heterogeneous degradation of Impact PP.

Pasch and co-workers [35] compared HT-HPLC, CRYSTAF and TREF results for the CCD of ethylene/acrylate copolymers and found a very good agreement. Wang et al. [36] studied the compositional heterogeneity, phase structure and melting behaviour of PP prepared by two spherical $TiCl_4/MgCl_2$ catalysts in reactor alloys by a combinatory investigation of NMR, TREF, DSC and SEM techniques. They found that a reactor alloy prepared by a complex ethylene/propylene copolymerization is composed of PP homopolymer, PE homopolymer, and ethylene-*co*-propylene copolymer with different ethylene segment lengths. Another sample was mainly composed of PP homopolymer, ethylene-propylene segmented polymer and ethylene-propylene random copolymer. Correlations between the molecular architectures, phase structures and the ultimate mechanical properties were constructed. SSF was compared with TREF by Godard and co-workers [37]. They concluded that the SSF method is a more suitable method to obtain large quantities of low-dispersity HDPE fractions over a wide range of molar masses. Buran et al. [38] studied the degradation of impact PP (ICPP) during processing by multiple extrusions using successive self-nucleation annealing (SSA), TREF, SEM and FTIR. They found that the ICPP behaved like PP homopolymer because PP constituted about 90% of the total sample mass. Degradation takes place mainly in the PP homopolymer phase. Although none of the techniques revealed an unambiguous description of the phenomena taking place in the rubbery phase, there were several indirect indications among them an increase in the average molar mass that pointed at cross-linking reactions in the rubbery phase.

Amer and van Reenen [39] fractionated isotactic polypropylenes by TREF to get fractions with different molar masses but similar tacticities. The DSC results of the fractions indicated that the crystallization behaviour is strongly affected by the configuration (tacticity) and the molar mass of the PP. Soares et al. [40] proposed a new approach for identifying the number of active catalyst sites and the polymer chain microstructural parameters produced at each active site for ethylene/1-olefin copolymers synthesized with multiple-site catalysts. This method is based on the simultaneous deconvolution of bivariate MMD/CCD, which can be obtained by cross-fractionation techniques like SEC/TREF or TREF/SEC. The proposed approach was validated successfully with model ethylene/1-butene and ethylene/1-octene copolymers. Alamo and co-workers [41] studied the effects of molar mass and branching distribution on mechanical properties of ethylene/1-hexene copolymer film grade resins produced by a metallocene catalyst. Molar mass fractions were obtained by solvent/non-solvent techniques while P-TREF was used for fractionation according to the 1-hexene content.

IR detectors operating at a single wavelength are commonly used as concentration detectors in TREF. This works well for simple copolymer systems but not for complex ones. Zhang [42] proposed to use FTIR detection for TREF analysis and demonstrated the power of this approach for three copolymer systems: ethylene/α-octene copolymers, polystyrene-grafted ethylene-vinyl acetate and ethylene/methyl acrylate copolymers. This online FTIR detection allows the simultaneous determination of polymer concentration and polymer composition avoiding time and labour consuming TREF fractionation and subsequent analysis by NMR. Fan et al. [43] characterized polypropylene-*g*-polystyrene by P-TREF and fractions were further characterized by ^{1}H- and ^{13}C-NMR, FTIR, SEC, DSC, and WAXD. They showed that the grafted PP fraction eluting at 114°C accounts for 42% of the bulk graft copolymer and has the highest degree of grafting, high melting temperature and crystallinity, and high molar mass. They concluded from their results that the grafted polymer contains a major component that has a low branching density and a high degree of grafting, and a minor component with a high branching density and short branches. Park and co-workers [44] synthesized ethylene/1-butene copolymers having different comonomer ratios with SiO_2-supported $TiCl_4$ catalyst. The products were characterized by TREF and CRYSTAF. TREF analysis showed that the copolymers had a broad and bimodal CCD regardless of the content of 1-butene in the copolymer. The SCB concentration was in the range of 5–55 branches/1000 carbons for all copolymers prepared in the study. Furthermore, the broader CCD was explained with the higher content of 1-butene in the copolymer. The peaks in the CRYSTAF curves appeared at lower temperatures than those of the TREF curve, resulting from the supercooling effect, similar to what could be observed between the heating and cooling cycles in DSC. This is because the CRYSTAF curve was measured during the process of crystallization, whereas TREF was measured during the process of melting and dissolution. In the case of a copolymer with a 1-butene content of 5.1 wt%, both TREF and CRYSTAF analysis showed a broadening of the peaks and a growing of the lower crystalline part. TREF gave a more prominent broad peak in comparison to the CRYSTAF curve (Fig. 5). CRYSTAF analysis did not show a bimodal CCD for the copolymers having a 1-butene content of less than 5.1 wt%. It was concluded that TREF gives more detailed and distinct information on CCD of copolymers in comparison to CRYSTAF in the lower comonomer content range of 0–5%.

Pasch and co workers [45] hyphenated TREF fractionation with SEC-FTIR to measure the compositional heterogeneity within a commercial impact PP copolymer and demonstrated successfully that the combination of TREF and SEC-FTIR provides a simple alternative to more time-consuming conventional ways of characterizing impact PP copolymers of complex heterogeneity. Hasan et al. [46] correlated the TREF, ^{13}C NMR and SEC results of PP produced by different Ziegler–Natta catalysts in terms of catalyst preparation method, polymerization conditions, type of co-catalyst, and evaluated the performance of the catalyst with respect to several aspects including the grinding effect on the surface catalyst performance, etc. Their results show that the polymerization activity, isospecificity and the isospecificity distribution of active sites of $TiCl_3$ catalysts are mainly

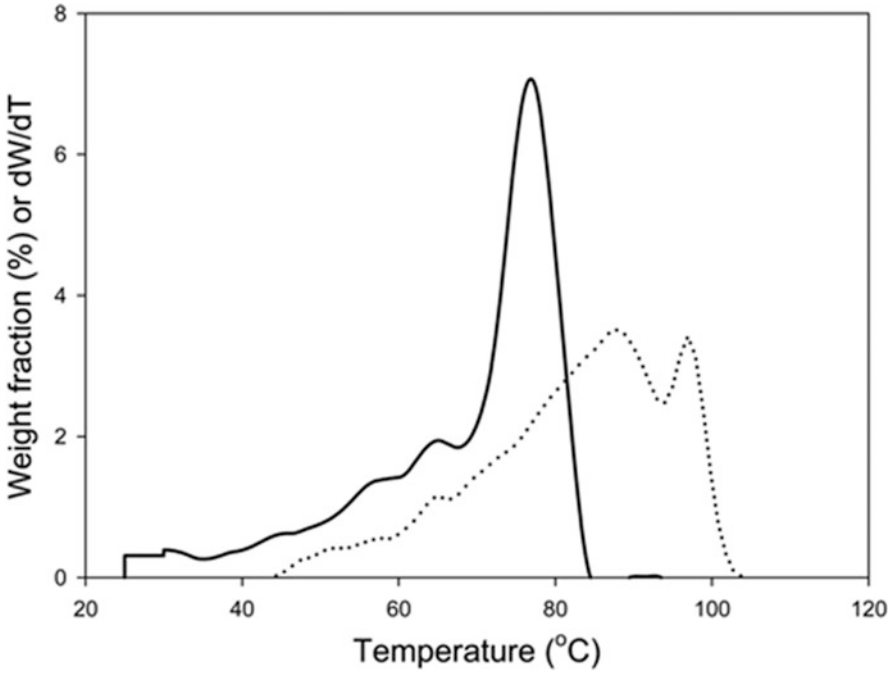

Fig. 5 Comparison of TREF and CRYSTAF curves for the copolymer having 1-butene content of 5.1 wt%; *dashed line* CRYSTAF, *dotted line* TREF. (Reprinted from [44] with permission of Springer Science + Business Media)

affected by the type of Al-alkyl co-catalysts. They demonstrated that the isospecific nature of surface Ti-species combined with the coordination state of surface Al-compounds completely replicates the polymer microtacticity. Kuhlman and Klosin [47] showed by TREF analysis that the block composition of polyethylene multiblock copolymers can be tuned by selection of a suitable catalyst system. The combination of soft and hard catalysts and diethylzinc (DEZ) as chain shuttling agent were used in this study to tune the block composition. The structures of catalysts are shown in Scheme 1. TREF data depict the effect of different catalyst systems on the final block composition (see Fig. 6).

The amorphous part of the samples is eluted at the lowest temperature as a narrow peak without a specific resolution of the components.

Helland and co-workers [48] fractionated LLDPE by P-TREF and preparative molar mass fractionation. They analyzed the fractions with SEC-FTIR, NMR and CRYSTAF and explored different ways of combining and processing the data to obtain two and three dimensional results. Bivariate distributions were obtained by using two approaches. Both approaches are based on fractions from preparative chemical composition fractionation analyzed with SEC and NMR. In the first approach CRYSTAF was in addition used to determine the CCD of each fraction. They name data from this approach $3D_{CRYSTAF}$. In the second approach CCD

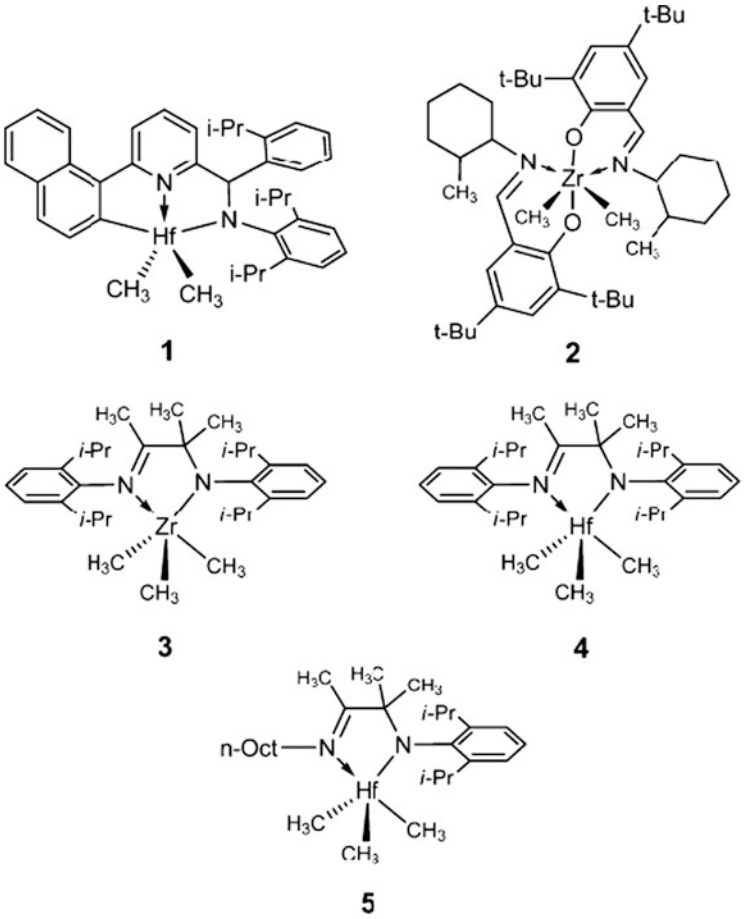

Scheme 1 Catalyst structures (Reprinted from [47] with permission of American Chemical Society)

information was calculated from the fraction sizes and end group content. This data set was named $3D_{fast}$ since it requires less analysis. Intuitively $3D_{CRYSTAF}$ should have better resolution, but, as was shown, the limitations of CRYSTAF makes $3D_{fast}$ better at some points. Despite its simplicity $3D_{fast}$ gave the best results. The problems encountered with CRYSTAF could possibly be eliminated by using the more precise but also more time consuming analytical TREF method. If lower accuracy is acceptable the $3D_{fast}$ approach can be speeded up further by performing CC analysis using FTIR instead of NMR. It is shown that cross fractionation discloses property relevant details, which are not disclosed by either CC or MM fractionation alone. They depicted the critical differences in distribution of comonomer at high MM that correlates with differences in impact strength and crystal structure. This information is valuable in material development and is not disclosed

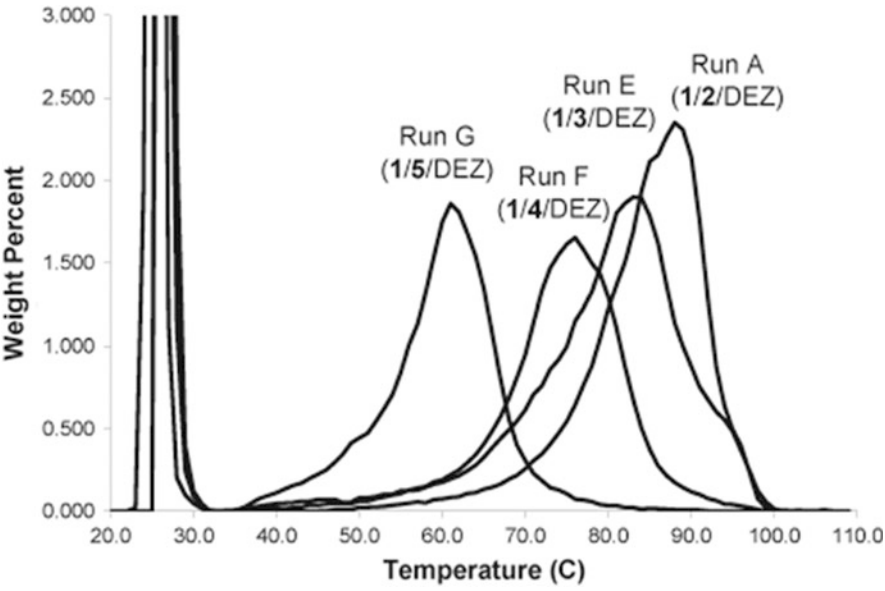

Fig. 6 Temperature rising elution fractionation (TREF) data for olefin block copolymers showing the influence of α-olefin content in the hard block on polymer solubility; sample code indicates catalyst composition. (Reprinted from [47] with permission of American Chemical Society)

by one-dimensional fractionation analyses. Many of the experimental procedures used in this investigation are labour intensive. The results of this work suggest SEC-FTIR and the $3D_{fast}$ approach as the methods delivering most valuable information compared to the required labour. More recently Harding and van Reenen [49] reported on the role of two different donors (diphenyldimethoxysilane and methylphenyldimethoxysilane) for the Ziegler–Natta catalyzed propylene polymerization. From TREF and SEC analyses they concluded that diphenyldimethoxysilane is a more efficient donor producing higher molar mass and lower polydispersity PP. The correlation between the molecular characteristics of the material and the properties was investigated.

2.2 Crystallization Analysis Fractionation

CRYSTAF was developed by Monrabal [50] as an alternative to TREF. Both techniques basically provide comparable results but TREF is the more time consuming process involving two steps, crystallization and elution, while CRYSTAF has only a crystallization step. CRYSTAF is based on the continuous crystallization of polymer chains from a dilute polymer solution. The concentration of the polymer in solution as a function of temperature is measured with a suitable detector like IR. As a result a concentration profile of the polymer in solution as a function of

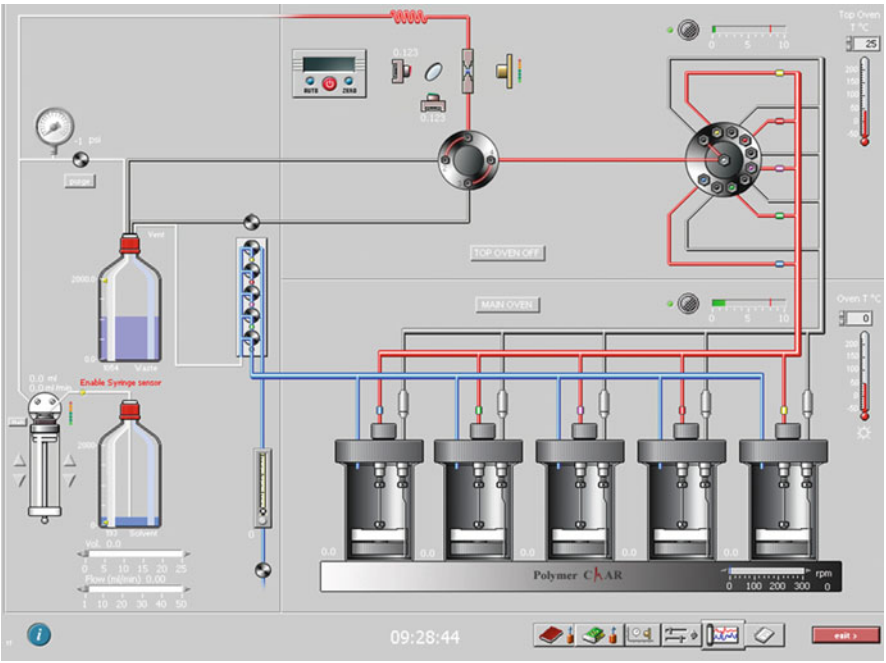

Fig. 7 Systematic diagram of a CRYSTAF instrument (Polymer Char, Spain) (screenshot from instrument)

temperature is obtained. With decreasing temperature an increasing fraction of polymer crystallizes out of solution and, therefore, the concentration in solution decreases. The concentration of the polymer at a given temperature is correlated with chemical composition (copolymer) through a calibration curve similar to the approach in TREF. The calibration curve is obtained for particular experimental conditions (cooling rate, comonomer type, solvent, etc.) based on copolymer standards with narrow CCDs. The polyolefins with narrow CCDs are typically obtained from P-TREF fractionation or directly by polymerization using single-site catalysts.

The commercial version of CRYSTAF from Polymer Char (Valencia, Spain) is shown in Fig. 7. It consists of five stirred stainless steel crystallization vessels that are placed in a temperature programmable oven and can be used for the simultaneous analysis of five samples. The vessels are connected to a nitrogen line, a waste line and a sampling line attached to an inline filter. The sampling line is connected to an online dual wavelength IR detector that is heated to 150°C to measure polymer concentration in solution as a function of temperature. The polymer sample (0.1–1.0 mg/mL) is dissolved in a good solvent such as TCB at a high temperature followed by a stabilization period slightly above the initial crystallization temperature. Higher and lower concentrations than the recommended ones could lead to either interchain interactions and co-crystallization or poor signal-to-noise ratio.

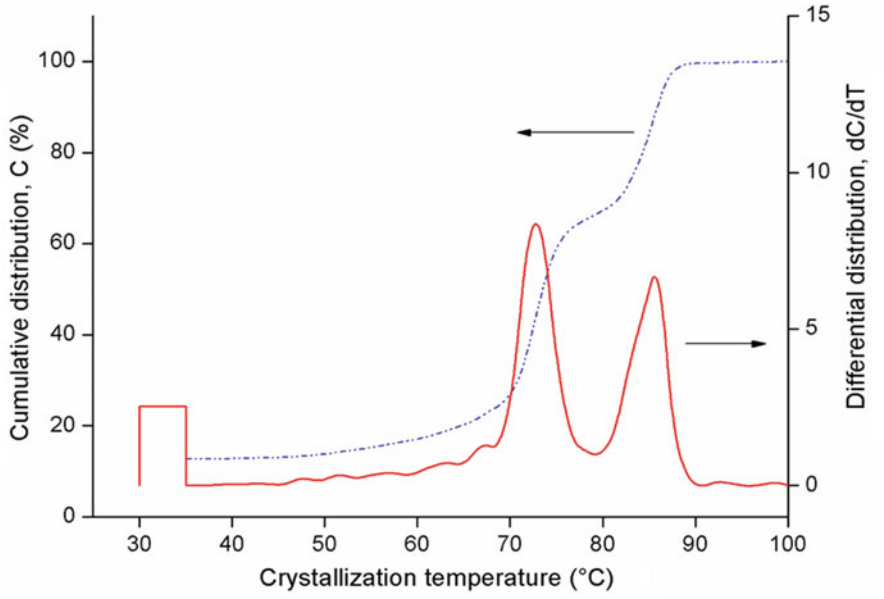

Fig. 8 Cumulative and differential CRYSTAF profiles of a blend of HDPE and PP

The recommended stirring rates are 200 rpm during dissolution and stabilization and 100 rpm during crystallization. The temperature of solution is decreased at a constant cooling rate (typically 0.1–0.2°C/min) during the crystallization step. The slow cooling rates are essential to avoid co-crystallization effects. Sample aliquots are taken out of the vessels at a given sequence and directed to the IR detector and the concentration of solution is recorded as a function of temperature. The plot of polymer concentration as a function of temperature (see Fig. 8) is called cumulative CRYSTAF profile.

The amount of the polymer crystallizing at each temperature can be obtained by differentiation of the integral CRYSTAF profile at each temperature. The plot of amount of polymer crystallized as a function of temperature is the most common and the clearest reporting method of CRYSTAF results. Both types of plots for a blend of HDPE and PP are shown in Fig. 8. Similar to TREF, there are several factors which can affect CRYSTAF profiles and the reliability of results including the molar mass of the polymer, the comonomer type and content, the cooling rate (CR), co-crystallization effects. Soares et al. wrote two comprehensive reviews about crystallization based techniques in 2005 [13, 51]. In this review we focus on the work that has been published more recently.

Gemoets and Hagen [52] derived a mathematical expression ψ for CRYSTAF curves to describe the longest ethylene sequence (LES) distribution of random copolymer chains. The comparison of the LES-distribution of a random copolymer having a polydispersity of 2, as calculated by $\psi_{polymer}$, with Monte-Carlo simulations and a method previously described in the literature showed that the derived

mathematical expression ψ is correct. This model allows for the description of the crystallizing temperature (CT) distribution of polymers using the reported relation between CT and LES. It will also hold if the CT of a chain would depend on other chain properties next to its LES. Weiser and Mülhaupt [53] synthesized and characterized a new phenoxyimine based catalyst and used this catalyst for the preparation of a PE-block-P(E-*co*-P) type copolymer. The material was characterized by CRYSTAF and AFM to check the efficiency of the catalyst in this olefin polymerization. Joubert and co-workers [54] reported the homogeneous tandem catalysis of a bis(diphenyl-phosphino)amine-chromium oligomerization catalyst with the metallocenes $Ph_2C(Cp)(9\text{-}Flu)ZrCl_2$ and rac-$EtIn_2ZrCl_2$. They discussed different influencing factors like polymerization temperature, reaction time, catalyst and co-catalyst ratios on the polymerization behaviour and on the properties of the final products. The products were characterized by a combination of different analytical techniques including CRYSTAF, ^{13}C NMR, and DSC. Weiser et al. [55] synthesized and characterized high molar mass PE-block-P(E-*co*-P) type block copolymers on a tailor-made phenoxyimine catalyst. The products covered the entire feasible range of chemical compositions. A systematic variation of the block length and the propylene content was performed. NMR, DSC, DMA, CRYSTAF and HT-HPLC were used to analyze the products and results showed that there is no homopolymer of either type formed during the synthesis of the block copolymers and the block copolymer composition is quite uniform. Monrabal [56] proposed a new approach to get more information out of single TREF and CRYSTAF runs by attaching additional detectors. The incorporation of light scattering and infrared composition detectors to TREF and CRYSTAF equipment provides additional information on the composition-molar mass dependence and adds to the identification of complex blends. Soares et al. [57] developed a new model for CRYSTAF analysis of polydisperse homopolymers. In this model, crystallization kinetics effects were taken into account which was not the case in previous models. Their model fitted the experimental CRYSAF profiles of four different polyethylene resins measured at a broad range of cooling rates. Their current model is theoretically sound and agrees with the values previously reported for similar systems. The model also describes MMD effects on CRYSTAF profiles. They depicted that the MMD effect is more pronounced for lower molar masses but can also be noticed for higher molar mass samples. Luruli et al. [58] synthesized ethylene/1-pentene copolymers using Cp_2ZrCl_2(1)/MAO and [$(CO)_5$ W = C(Me)OZr$(Cp)_2$Cl] (2)/MAO catalyst systems. They have used a combination of several analytical techniques like SEC, DSC, FTIR, ^{13}C NMR and CRYSTAF to analyze the products and correlate the findings with the efficiency of the catalysts used. Soares et al. [59] investigated the influence of different catalyst supports on the catalytic activity of metallocenes by preparing ethylene/1-hexene copolymers. All the poly(ethylene-*co*-1-hexene) samples made with $(nBuCp)_2ZrCl_2$/MAO supported on SiO_2, SiO_2/Al_2O_3, MCM-41 or SBA-15 had narrow MMD but CCDs that varied from narrow and monomodal to broad and bimodal. The CCDs of copolymers made with $(nBuCp)_2ZrCl_2$/MAO supported on SiO_2 and SiO_2/Al_2O_3 were always unimodal, but those made with MCM-41 and SBA-15 became bimodal with increasing 1-hexene content. This bimodality may be related to the presence of two catalyst site types on the

surface of the support. Lower CRYSTAF temperature peaks (that is, polymer populations with higher 1-hexene fractions) became more prominent with decreasing Si/Al ratio, and larger pore sizes seemed to favour the 1-hexene incorporation. This investigation demonstrates that copolymer samples that do not differ significantly in their MMD shapes can have totally different CCD profiles as measured by CRYSTAF. Therefore, the authors argue that CRYSTAF (or equivalently TREF) is an essential analysis tool to characterize copolymers made with coordination catalysts, even when they are expected to behave as single-site catalysts. Soares et al. [60] investigated three different ethylene/1-hexene copolymers with different 1-hexene contents but similar number average molar masses at several cooling rates for CRYSTAF analysis. They proposed a mathematical model to describe the effect of comonomer fraction and cooling rate on CRYSTAF fractionation. They successfully extended their previous model which accounts for effects of crystallization kinetics and MMDs for polyethylenes and binary ethylene/1-olefin copolymers. Van Grieken et al. [59] tested the catalytic system $(nBuCp)_2ZrCl_2$/MAO immobilized over SiO_2–Al_2O_3 in ethylene/1-hexene copolymerizations using different amounts of comonomer. The products were analyzed by ^{13}C NMR, SEC, CRYSTAF and DSC. They showed that the catalytic activity increases with comonomer concentration up to 0.194 mol/L. This was related to better monomer diffusion. The decrease in catalyst activity at higher concentrations is due to a lower insertion rate of larger comonomers in the polymer chains. They also showed that after a polymerization time of 20 min the incorporation of 1-hexene decreases because of larger mass transfer limitations. Therefore, the CCD during the first minutes of reaction is broader with a maximum at lower temperature corresponding to 1-hexene-rich fractions while as the polymerization time increases the CCD curves became narrower with a maximum shifted towards higher temperatures as a result of the formation of ethylene-rich fractions. Kissin et al. [61] developed a computerized method for quantifying CRYSTAF data based on resolution of CRYSTAF curves. This analysis of CRYSTAF curves gives three parameters characterizing crystallizable polymer material: (a) the number of compositionally uniform components, (b) properties of each compositionally uniform component, and (c) the quantity of each component. The ethylene/1-hexene copolymers produced by Ziegler–Natta catalysts showed the existence of two distinct groups of copolymer contents that contain lower and higher comonomer contents. The higher comonomer content component precipitates at much lower temperature as a broad overlapping group of peaks in contrast to the component with low comonomer content that precipitates at higher temperatures as several relatively sharp peaks. Islam et al. [62] studied the effects of branching content and copolymer composition distribution on the non-isothermal crystallization kinetics of metallocene based m-LLDPEs using modified Avrami analysis, modulated differential scanning calorimetry and CRYSTAF. They have shown that the absolute crystallinity decreases with increasing comonomer content and vice versa. Soares et al. [63] analyzed a series of ethylene homopolymers and ethylene/1-hexene copolymers with different molar masses and chemical composition distributions by CRYSTAF at several cooling rates. The effects of MMD, CCD and cooling rates on the CRYSTAF profiles were investigated. Using their results, a mathematical model was developed for CRYSTAF that considers the

kinetics of crystallization. They fitted the model successfully to experimental results. The model describes well how molar mass and comonomer content affect the CRYSTAF profiles of polyethylene and ethylene/1-olefin copolymers.

Macko et al. [64] analyzed graft copolymers of propene and styrene regarding chemical heterogeneity by SEC coupled with FTIR and CRYSTAF. The results showed that the PP-*g*-PS copolymers have a well defined homogenous graft structure. The decrease in crystallization temperature in CRYSTAF did not correlate with the concentration of PS in the sample but with the branching frequency. Furthermore, the length of branches did not influence the CRYSTAF profiles. Kissin and coworkers [65] presented kinetic data on ethylene homopolymerization and ethylene/1-hexene copolymerization with two types of chromium oxide catalysts. The products had broad molar mass and chemical composition distributions. A combination of kinetic data and structural data of the copolymers provided detailed information about the frequency of chain transfer reactions for several types of active centres present in the catalyst, their copolymerization efficiency and stability.

Soares et al. [66] developed a new methodology to construct the CRYSTAF calibration curves (crystallization temperature vs. copolymer composition) using a crystallization kinetics model. The results of simulation agreed quite well with experimental data and the estimated CCDs were consistent with theoretical predictions from Stockmayer's distribution. The effects of cooling rates, comonomer type and molar masses were quantified successfully with their proposed model. In another report by Terano et al. [67] ethylene homopolymers and copolymers (with cyclopentane) synthesized by Phillips Cr(VI)Ox/SiO_2 catalysts were investigated for solution crystallization behaviour. Remarkably they found that the crystallization peak temperatures of these polymers increased with increasing cyclopentene reactor concentration from 0 to 20 vol%. The authors assume that the decreasing SCB frequency was the dominant factor to explain the increasing crystallization peak temperature. Soares and co-workers [68] used a Monte Carlo model to predict microstructure details of olefin block copolymers (OBC) and a modified version of their previously proposed CRYSTAF model was used to describe the theoretical results. The model was used as a tool to interpret CRYSTAF results and these results were correlated to microstructures and polymerization parameters. The authors suggest that their model can be used in the future to examine the effect of polymerization parameters on OBC microstructure. Based on the attained knowledge, the process conditions could be fine-tuned to prepare OBCs with the desired chain microstructure and properties. Alghyamah and Soares [69, 70] developed a new procedure to deconvolute the MMD and cumulative CCD of polyolefins made by heterogeneous Ziegler–Natta catalysts. Their mathematical algorithm uses Flory's most probable distribution and Stockmayer's distribution simultaneously to deconvolute MMD and CCD. It was shown that their model can be applied to several industrial polyolefins to estimate the number of active sites, the number average molar mass, the average comonomer fraction and the mass fraction of soluble and non-soluble polymer made on each catalyst site in an accurate and repeatable way. Anantawaraskul and Chokputtanawuttilerd [71] developed an artificial neural network (ANN) with a 4-3-3-1 architecture (i.e., four

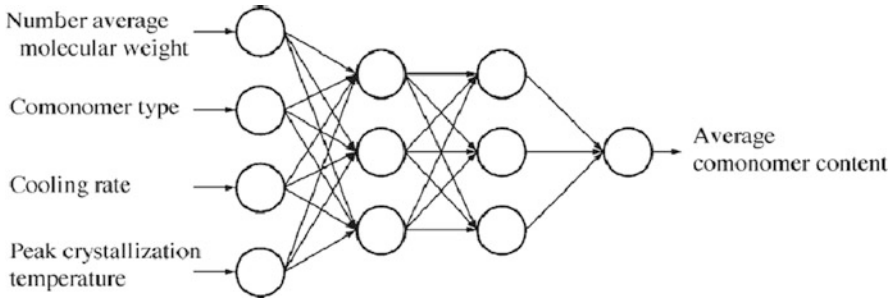

Fig. 9 ANN with a 4-3-3-1 architecture. (Reprinted from [71] with permission of Wiley-VCH)

input neurons, two hidden layers each with three neurons, and one output neuron) (see Fig. 9) to estimate average comonomer contents of ethylene/1-olefin copolymers from CRYSTAF results. It was shown that the average comonomer contents predicted by AAN are in good agreement with experimental results and AAN can be a useful tool in interpreting CRYSTAF results.

Macko et al. [72] demonstrated that the CRYSTAF apparatus with some modifications has the potential to be a widely applicable instrument for studying adsorption phenomena of small molecules as well as macromolecules in various solvent-sorbent systems. The adsorption isotherms of PE adsorbed from TCB on a zeolite were experimentally determined. Aust and co-workers [73] demonstrated that the coupling of a mathematical model and experimental investigations is an efficient way of finding significant experimental operating parameters and interactions of a CRYSTAF measurement process. The results reveal that the precipitation of polymer blends from the solution is strongly influenced by the acceleration field in a radial direction during the precipitation process. In CRYSTAF analysis the phase separation quality of RACO (polyolefin blends consisting of a random PP copolymer)-PE blends is mainly controlled by the stirring speed for the cooling rate interval of 0.1–0.3°C/min. On the basis of their findings they developed an optimized CRYSTAF characterization method and experimentally verified it with three different blends. Gao et al. [74] combined results of CRYSTAF, SEC and ^{13}C NMR to study the effects of diisobutyl phthalate (DIBP) and 2,4-pentadiol dibenzoate (PDDB) as internal donors for the $MgCl_2$-supported catalysis of propylene polymerization. The performance of the catalyst was compared with other catalysts containing donor-free DIBP and PDDB as internal donors. Their results show that the catalyst containing internal donors had high activity, stereoselectivity and gave a relatively broad molecular weight distribution of the resulting polymer, which might be ascribed to the synergistic effect between PDDB and DIBP. Most recently Monrabal and Heirro [75] demonstrated that the use of only TREF or CRYSTAF for polyolefin analysis can be equivocal. TREF results are more reliable for combinations of highly regular isotactic polypropylene and polyethylene. CRYSTAF is the preferred technique when analyzing combinations of polyethylene with EPC or less regular polypropylene resins. To obtain unequivocal results for complex polypropylene and/or polyethylene combinations, both TREF and CRYSTAF must be considered.

2.3 Crystallization Elution Fractionation

Recently a fascinating new development in crystallization based techniques for CCD analysis of semicrystalline polyolefins has been published. This new technique is called CEF. As demonstrated by Monrabal and Heirro [75] the use of only TREF or CRYSTAF for polyolefin analysis might lead to equivocal results and the use of both techniques for unequivocal results was recommended. CEF is an important step forward in this direction and it combines the separation power of TREF and CRYSTAF in one single fast run.

Figure 10 demonstrates the differences between normal TREF, dynamic crystallization and CEF. Figure 10a depicts the typical TREF process. The first step in all cases would be sample loading and in TREF this is followed by typical crystallization and elution steps as explained in detail in Sect. 2.1. The first step in dynamic crystallization (Fig. 10b) is the same sample loading and the second crystallization step is performed with a small solvent flow through the column during slow cooling. The fraction which reaches crystallization temperature segregates and anchors on the support while other components in solution move along till they reach their crystallization temperature. This allows the physical separation of the fractions according to crystallizability within the column in the crystallization cycle. The flow rate during the crystallization cycle is a very important factor to

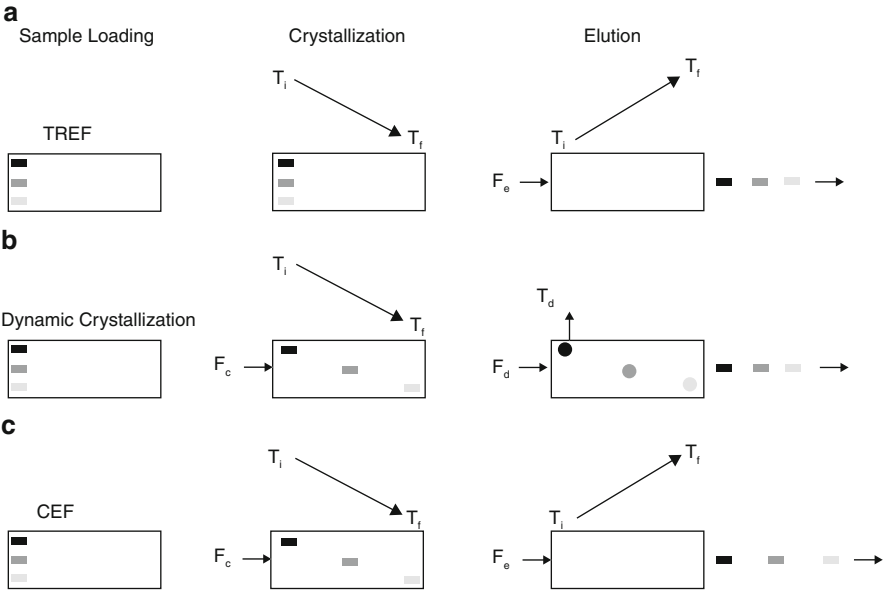

Fig. 10 Separation diagram by crystallizability. (**a**) TREF separation process, (**b**) dynamic crystallization, (**c**) crystallization elution fractionation. (Reprinted from [76] with permission of Wiley-VCH)

achieve better separation. Once the crystallization cycle is completed, the flow through the column is stopped and the column is heated to higher temperatures for a few minutes where all the components dissolve again. The flow of solvent with an appropriate flow rate is started again to elute all different fractions. CEF combines the two processes explained in Fig. 10a, b. The first step is the sample loading step which is the same for all three methods while step one (crystallization) from dynamic crystallization (Fig. 10b) and step three from TREF (Fig. 10a) are combined to enhance the resolution power. The third step of dynamic crystallization is basically replaced by a typical TREF elution cycle (see Fig. 10c). This allows an enhanced resolution of fractions in shorter times, giving better results. The schematic diagram of the combined CEF, dynamic crystallization and TREF instrument is shown in Fig. 11.

Monrabal et al. [76] proposed this new approach which combines separation power of CRYSTAF and TREF and provides very fast analysis in comparison to long analysis times of other crystallization based techniques. CEF can be performed in a typical column based TREF instrument and can easily adapt viscometry, light scattering, composition or other molar mass sensitive detectors. In another paper, Monrabal et al. [77] demonstrated that dynamic crystallization analysis can be optimized by knowing the crystallization range of the sample and adapt the experimental conditions accordingly. CRYSTAF and dynamic crystallization

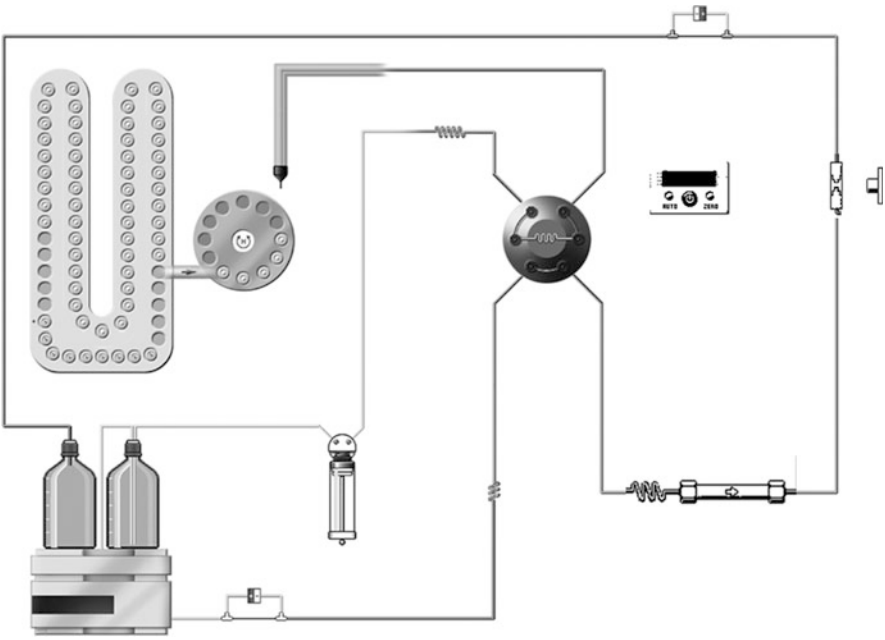

Fig. 11 Schematic diagram of the combined CEF, dynamic crystallization and TREF instrument. (Reprinted from [76] with permission of Wiley-VCH)

(DC) results obtained using the same cooling rates provided comparable results. The extended separation power of CEF over TREF comes from the extra separation in the DC step and, therefore, the optimization of the DC step has a significant impact on CEF optimization. They also proposed a new approach to reduce co-crystallization by using multiple crystallization elution cycles. It was shown that co-crystallization can be minimized and resolution can be improved by increasing the number of cycles. Hermel-Davidock et al. [78] used samples with very different molar masses and densities to explore the influence of molar mass on the CCD of bicomponent systems by using CEF and CRYSTAF. The study demonstrated the ability of triple detector CEF to deconvolute the CCD profile of bicomponent systems which was not achievable by conventional CRYSTAF. The advantage of triple detector CEF is a result of the large number of data points collected along the temperature profile, high resolution and reproducibility. Soares et al. [79] showed more recently by using different blends of ethylene/1-octene copolymers the effect of chain crystallizabilities, blend composition, and cooling rate on the extent of co-crystallization in CRYSTAF and CEF. The extent of co-crystallization in both methods increases in any of the situations: (1) the chain crystallizabilities are close, (2) one of the blend components is present in large excess, and (3) fast cooling rates are used. However, they concluded that CEF was found to be more robust and have less co-crystallization than CRYSTAF. CEF also requires much shorter analysis times to achieve peak resolutions that are comparable with CRYSTAF and is well suited to high-throughput CCD characterization.

3 Column Chromatographic Techniques

3.1 Size Exclusion Chromatography

SEC is the premier polymer fractionation method for determining MMDs. In SEC, the separation mechanism is based on molecular hydrodynamic volume. The majority of polymers are soluble in organic or aqueous solvents at ambient temperature and SEC experiments are conducted at ambient or slightly increased temperatures [5, 6, 80].

Most polyolefins are semi-crystalline materials with melting temperatures above 100°C. They are resistant to most solvents and, indeed, do not dissolve at ambient temperature. Most polyolefins dissolve only at temperatures above their melting temperatures and require specific high-boiling point solvents. The full dissolution of polyolefins is usually achieved at temperatures between 130 and 160°C. Various solvents for the dissolution of polyolefins were proposed, among them tetrachloroethylene, decalin, α-chloronaphthalene, 1,2-dichlorobenzene, TCB, methylcyclohexane [81], cyclohexane [82–84] and TCB being most frequently used for SEC of polyolefins. Typical stationary phases are polymeric materials based on cross-linked polystyrene (PS-DVB gels). Various dissolution procedures

are used. Generally, a dissolution time between 1 and 6 h at a temperature of 150–180°C is recommended. During the dissolution process, the sample may be shaken or stirred [85–88]. For protection against thermo-oxidative degradation, phenolic antioxidants (e.g., butylated hydroxytoluene) are usually added in concentrations of 0.2 mg/mL [87] up to 1.5 mg/mL [88] to the solvent. Care must be taken to avoid the presence of oxygen, vigorous stirring and sample filtering because this may lead to sample degradation. Polyolefin chains may degrade during sample preparation or during the SEC separation itself [85, 86, 89]. The thermo-oxidative degradation and the chain scission due to shear stress in the SEC column are the main sources for the potential reduction of the polyolefin molar masses [85, 87].

Despite such experimental complications, HT-SEC is routinely used to determine the MMD of polyolefins [3, 4]. The corresponding high-temperature chromatography instruments have been commercially available since 1964. The instruments may be equipped with different detectors such as refractive index, viscometer, light scattering or infrared. Since HT-SEC for instrument producers is rather a niche market there are only a few types of instruments that are most commonly used including the Agilent PL-GPC 220 (www.chem.agilent.com/en-US/. . ./lc/gpc. . ./pl-gpc220), the Malvern/Viscotek HT-GPC (www.malvern.com/ViscotekHT-GPC) and the GPCIR of Polymer Char (www.polymerchar.com/gpc-ir).

HT-SEC is a reliable, precise, and fast method to measure the molar mass averages, the polydispersity index and the complete MMD of polyolefins. Depending on the complexity of the sample to be analyzed, there are several techniques that mainly differ by the added detectors and calibration options [90]:

(1) Conventional HT-SEC with a concentration detector (RI, IR, ELSD) and a narrow/broad/integral calibration curve constructed from matching molar mass reference standards and the sample.
(2) HT-SEC-light scattering with a concentration detector and a light scattering detector. If only a RALLS (right angle 90° laser light scattering) detector is available, in most cases a viscometer is needed to overcome the limitations of 90° light scattering (triple detection approach).
(3) HT-SEC-viscometry with a concentration detector and a viscometer, and a universal calibration curve constructed from any molar mass reference standards and materials.

Frequently a triple-detector SEC technology is used, where three on-line detectors are used together in a single SEC system. In addition to the concentration detector, an on-line viscometer and a MALLS instrument are coupled to the SEC (TriSEC). With TriSEC, absolute molar mass determination is possible for polymers that are very different in chemical composition and molecular conformation. The usefulness of the TriSEC approach has been demonstrated in a number of applications [91–95].

The combination of SEC and molar mass-sensitive detectors is a powerful tool for the analysis of complex polymers. It is, however, important to distinguish between claimed vs. actual capabilities and between potential expectations and demonstrated performances [96]. Two tables, taken from a critical review of

Table 1 SEC analysis using molar mass-sensitive detectors

Method	Information content	
	Primary	Secondary
Regular SEC		MMD
SEC-LALLS	MMD	
SEC-MALLS	MMD	RGD
SEC-VIS	IVD	MMD, RGD, copolymer M_n
SEC-VIS-LS	IVD, MMD, RGD	Copolymer M_n

MMD molar mass distribution, *IVD* intrinsic viscosity distribution, *RGD* radius of gyration distribution

Table 2 Generalization of molar mass-sensitive detectors

Intended measurements	LALLS/MALLS	Viscometer
MMD	Requires precise n and dn/dc, not affected by non-exclusion effects	Requires universal calibration and K, a-parameters
IVD	–	Directly from experiment, not affected by non-exclusion effects
RGD	MALLS only	Calculated from $[\eta]M$
Chain conformation and branching	R_g vs. M plot, MALLS only	$[\eta]$ vs. M plot, R_g vs. M plot
Chemically heterogeneous polymer analysis	Limited	Better
Noise, particulates, bubbles	Strongly affected	Less affected

different techniques, summarize the information content and additional details of SEC-light scattering and SEC-viscometry coupling [97]. The information content is classified into two categories: "primary" information is of high precision and accuracy, insensitive to SEC operation variables, and not requiring molar mass or universal calibration; "secondary" information is less precise and requires calibration; see Tables 1 and 2.

3.1.1 Coupled SEC-FTIR

For a detailed analysis of olefin copolymers or polyolefin blends it is important to determine the CCD in addition to the MMD. The bulk chemical composition of polyolefins can be determined quantitatively by FTIR or NMR spectroscopy. Dual information on the chemical composition as a function of molar mass can be obtained when HT-SEC is directly coupled to these spectroscopic methods. Interfacing SEC with ^{1}H-NMR is a cost-intensive option for the understanding of molecular structure as a function of separation. It has, however, the advantage

Table 3 Typical characteristics of flow cell and solvent-elimination interfaces for HPLC

Conditions	Flow cell	Solvent elimination
Gradient separation	No	Yes
Qualitative information	Limited, depends on eluent	Yes
Quantitative information	Excellent	Limited
Sensitivity	Moderate	Excellent
Eluent dependence	High	Low, eluent is eliminated before FTIR
Signal-to-noise ratio	Moderate, spectra collection on the fly	High, post-run scanning possible
Ease of operation	User friendly	Time-consuming optimization
Application area	SEC, isocratic HPLC	All LC methods

that the intensities of the NMR signals represent the concentrations of the protons of a certain species and no standards are required for quantification.

The coupling of LC techniques with FTIR is an important complementary technique. Because of the robustness, the simplicity and the cost effectiveness, LC-FTIR is the method of choice in most applications. The hyphenation of LC and FTIR can be realized in two ways: (1) on-line mode via a flow cell [98–101] and (2) off-line mode via a solvent elimination interface. The typical characteristics of the two approaches are summarized in Table 3 [102].

The application of flow cells has two major disadvantages. Most of the mobile phases that are used in polymer SEC exhibit strong absorptions in the mid-infrared region and thus excessively overlap with the IR signals of the analyte. Therefore, mobiles phases are required that have a very low absorption at the IR frequency of interest. The second disadvantage is that spectra are collected on the fly. Therefore, multiple scans to increase sensitivity cannot be taken in most cases.

As pointed out, a major limitation of all flow-through cells is the limited selection of solvents/mobile phases that exhibit sufficiently large spectral windows for high-sensitivity measurements. One of the few very fortunate cases is the SEC-FTIR analysis of polyolefins. In this case TCB is used as the mobile phase which is sufficiently transparent in the range of 2,700–3,000 cm^{-1} that is used for polyolefin detection. Alternatively, ODCB or tetrachloroethylene may be used. As has been shown by DesLauriers and others, the compositional heterogeneity (SCB) in polyolefins can be analyzed sensitively by on-flow SEC-FTIR [103–109]. Chromatograms are generated from ratio-recorded transmittance spectra where the spectrum of the pure mobile phase is used as background. Typical sample concentrations are 1–3 mg/mL and rather large injection volumes of 400–1,000 μL are used for sufficient signal-to-noise ratio. In the case of low density materials branching is determined as the levels of methyl (2,958 cm^{-1}) and methylene endgroups (2,928 cm^{-1}) [103, 104, 106]. For high density materials with low degrees of branching, multivariable statistical techniques are preferred [108].

A typical analytical result is shown in Fig. 12 comparing Ziegler–Natta catalyzed ethylene-1-hexene resins with high and low comonomer levels [109]. The degree of branching is given as “branches per 1,000 total carbons”. Similar

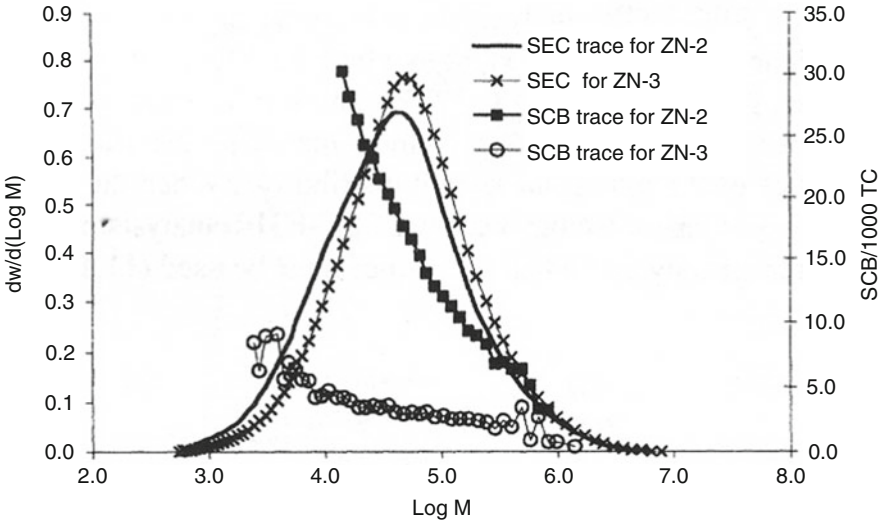

Fig. 12 SEC-FTIR analysis of LLDPE, comparison of comonomer incorporation in Ziegler–Natta catalyzed ethylene-1-hexene resins using high (ZN-2) and low (ZN-3) comonomer levels. (Reprinted from [109] with permission of American Chemical Society)

approaches can be used for other polymers provided that a spectral window is available for selective detection of the polymer species. Piel et al. [110] have recently significantly increased the signal-to-noise ratio in SEC-FTIR after application of a bandpass filter instead of a steel mesh attenuator and by changes in data processing. The signal obtained with the bandpass filter was almost four times higher than that obtained with the steel mesh attenuator. They used the proposed method for the determination of short-chain branching. Apart from SEC other fractionation techniques can also be applied such as analytical temperature rising elution fractionation (A-TREF).

A rather broad applicability of FTIR as a detector in liquid chromatography can be achieved when the mobile phase is removed from the sample prior to detection. In this case the sample fractions are measured in the pure state without interference from solvents. The breakthrough towards a powerful FTIR detector was achieved by Gagel and Biemann who formed an aerosol from the effluent and sprayed it onto a rotating aluminium mirror. The mirror was then deposited in an FTIR spectrometer and spectra were recorded at each position in the reflexion mode. This principle is used in an interface that originally was developed by Lab Connections Inc. introducing the LC-Transform [111–113] and modified further several times [114]. The LC-Transform system is a direct SEC-FTIR interface. The design concept of the interface is shown in Fig. 13. The system is composed of two independent modules, the sample collection module and the optics module. The effluent from the liquid chromatography column is split, with a fraction going into an ultrasonic nebulizer nozzle located above a rotating sample collection disc.

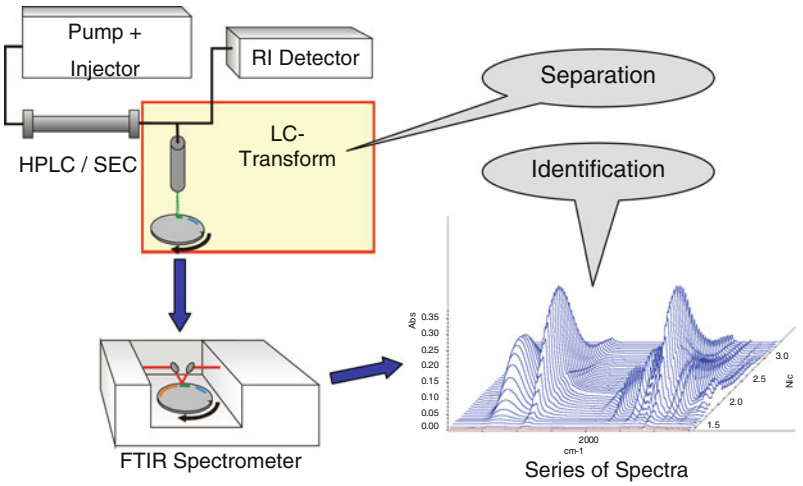

Fig. 13 Schematic representation of the universal SEC-FTIR coupling using the LC transform Interface

The nozzle rapidly evaporates the mobile phase while depositing a tightly focused track of the solute. When a chromatogram has been collected on the sample collector disc, the disc is transferred to the optics module in the FTIR instrument for analysis of the deposited sample track. A control module defines the sample collection disc position and rotation rate in order to be compatible with the run time and peak resolution of the chromatographic separation. The sample collection disc is made from germanium which is optically transparent in the range 6,000–450 cm^{-1}. The lower surface of the disc is covered with a reflecting aluminium layer [115].

As a result of the investigation a complete FTIR spectrum for each position on the disc and, hence, for each sample fraction is obtained. This spectrum bears information on the chemical composition of each sample fraction. The set of all spectra can be arranged along the elution time axis and yields a three-dimensional plot in the coordinates elution time-FTIR frequency-absorbance. Another way of representation is a diagram, where the content of one component in the copolymer is plotted across the molar mass axis.

As an example, the analysis of a blend of two EPDM copolymers with different molar masses and chemical compositions is presented in Fig. 14 [116]. The FTIR spectrum of an EPDM copolymer is given in Fig. 14a. The propylene percentage is determined from the absorption peak at 1,378 cm^{-1}, while the ethylidene norbornene is determined from the peak at 1,690 cm^{-1}. The percentage of the two monomers across the molar mass axis is given in Fig. 14b. As can be clearly seen, the propylene content of the higher molar mass copolymer is lower [116].

Using this experimental set-up, a multitude of different materials can be analyzed, including α-olefin copolymers, and polyolefin blends. In addition to the analysis of macromolecular components, the technique can be used for the detection and quantification of additives.

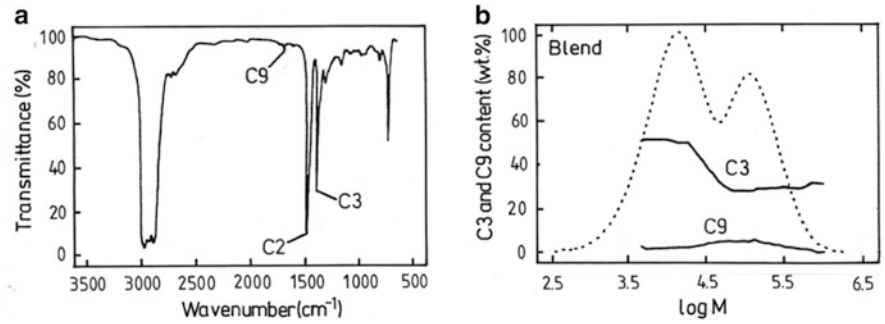

Fig. 14 FTIR spectrum of an EPDM copolymer (**a**) and HT-GPC/FTIR analysis of the blend of two EPDM copolymers (**b**)

Over the last few years a number of applications on the analysis of olefin copolymers have been published that make use of the LC-Transform system. These include the SEC-FTIR analysis of ethylene/vinyl acetate copolymers [117], ethylene/methyl methacrylate copolymers [118, 119], ethylene/styrene copolymers [120], HDPE and PP [121]. A number of studies used SEC-FTIR for monitoring the thermo-oxidative degradation of polyolefins [122–126] and a combination of TREF and SEC-FTIR to investigate the complex structure of olefin copolymers [127, 128].

The challenges for further improvement in sensitivity are to overcome the loss of IR sensitivity in the reflectance mirrors of the optic module and to deposit the effluents in rather narrow traces on the substrate. The configuration of the DiscovIR-LCTM interface, which was recently commercialized by Spectra Analysis Inc. (Marlborough, MA, USA), accounts for the energy loss in the optics module by using IR microscopy [129]. The instrument is a single unit that eliminates the solvent from the eluate received from the LC system and deposits the chromatogram as a track, which is a function of retention time. The track is scanned with a built-in FTIR microscope in real time. The deposition occurs under high vacuum and low temperatures (−140 to 100°C), which protects the compounds from oxidation. The deposition matrix is ZnSe and allows measurements in the transmission mode. A number of applications have been presented, however, none for the analysis of polyolefins.

3.1.2 Coupled SEC-^{1}H-NMR

Another most exciting new tool for the analysis of complex polyolefins is the direct coupling of high-temperature liquid chromatography and ^{1}H-NMR. Such equipment became available only recently when a high-temperature flow-through NMR probe was introduced by Bruker. The construction and experimental setup of the LC-NMR coupling is described in detail by Hiller et al. [130]. In brief, the NMR flow probe can operate at temperatures up to 150°C. The probe has an active flow cell with a volume of 120 μL. It is a dual inverse ^{1}H/^{13}C probe with pulse field

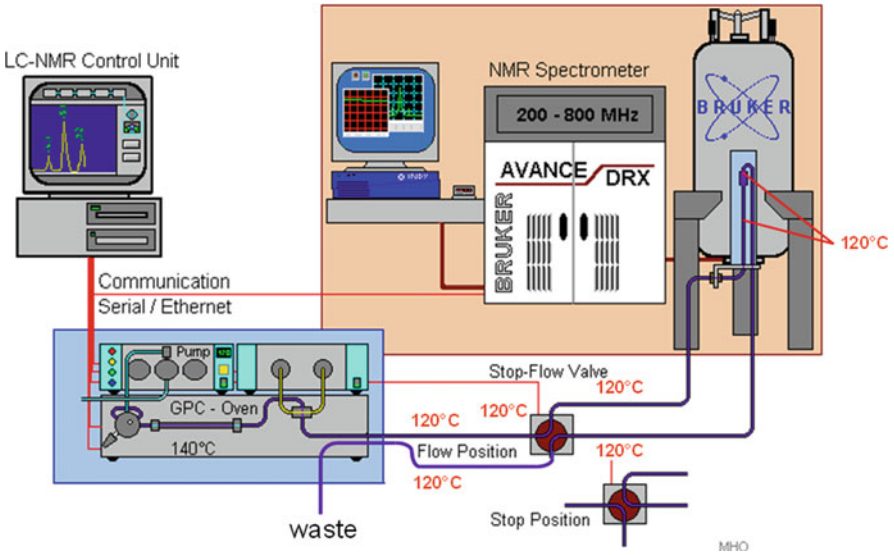

Fig. 15 Experimental setup of the high temperature SEC-NMR (SEC: 130°C; LC probe, stop-flow valve and transfer lines: 120°C). (Reprinted from [130] with permission of Elsevier Limited)

gradients. A stop-flow valve was developed as an interface for the SEC and the NMR. The valve is a two position device and guides the flow either from the SEC to the NMR or directly to the waste; see Fig. 15. This setup allows on-flow experiments, automatic stop-flow experiments and time-slicing.

To evaluate the capabilities of the system, a polymer blend comprising PE and PMMA homopolymers and a PE/PMMA copolymer was prepared and analyzed. The molar masses of PE, PMMA and the copolymer were $M_n = 1{,}100$ g/mol, $M_n = 263{,}000$ g/mol and $M_n = 10{,}600$ g/mol, respectively. The experiments were performed with TCB as the mobile phase. WET suppression was applied to the intrinsic solvent signals, i.e., the three aromatic proton signals were suppressed.

Figure 16 shows the on-flow run of the blend as a corrected contour plot by subtracting signals, which correspond to impurities of the solvent. In the SEC system the elution of the blend components is in the order of decreasing molar mass. This elution order can be clearly seen in the SEC-NMR contour plot. The spectra of the early eluting fractions show signals for PMMA but not for ethylene. In contrast, the late eluting fractions exhibit signals for ethylene but not for MMA and can be assigned to PE. Between the two homopolymers, the elution of the copolymer can be measured by detecting signals for both MMA and ethylene. Figure 16 also shows the vertical projections taken from the sum of the NMR signals. It can be used as the chromatogram which also indicates three separated peaks.

Figure 17 shows the different traces of the on-flow experiment. These traces clearly indicate the different components of the blend. The signals of the PMMA

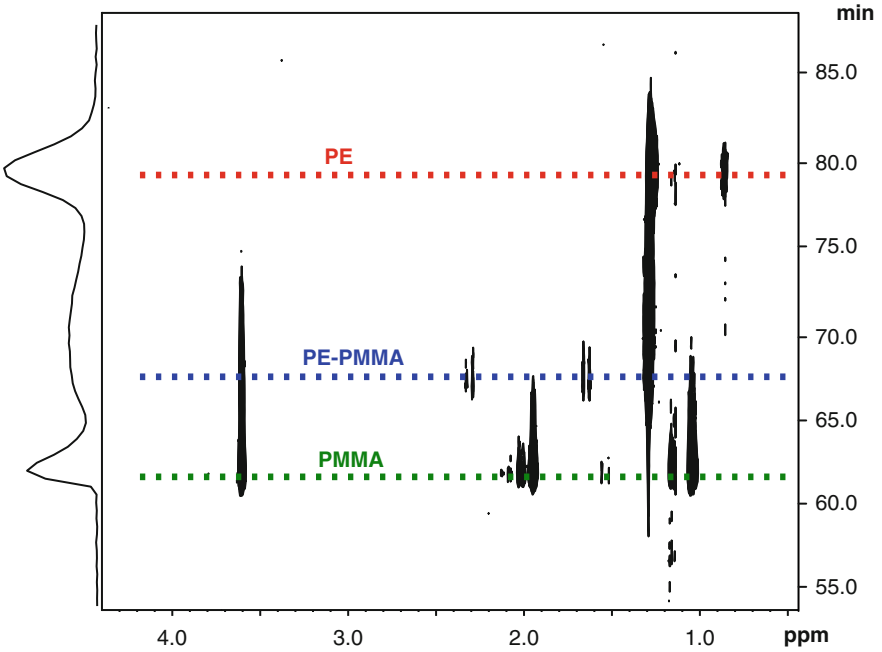

Fig. 16 SEC-NMR (400 MHz) on-flow run (corrected) of a PE–PMMA-copolymer blend at 130°C in TCB. (Flow rate 0.5 mL/min, concentration 2 mg/mL of each polymer, 300 µL injection volume, 5 Waters columns, 24 scans per FID, 1.24 s repetition delay.) (Reprinted from [130] with permission of Elsevier Limited)

(a) correspond to syndiotactic species of this homopolymer. The second trace (b) contains the copolymer. It is a block copolymer where MMA is mainly isotactic. The third trace contains only the PE component. It even shows the CH_3 end group at 0.86 ppm. However, the signal-to-noise ratio of the CH_3 group is not sufficient for a precise molar mass calculation.

In the second experiment, the CCD of the PE/PMMA copolymer was investigated by using on-flow and stop-flow experiments. The distributions of the different structural moieties corresponding to MMA and ethylene can be seen and correlated with the corresponding molar masses. The quantification of the chemical composition based on the on-flow data is presented in Fig. 18. It shows that the MMA monomer units are mainly distributed at higher molar masses.

Recently, a new cryoprobe for high-temperature NMR has been introduced. This cryoprobe enables a dramatic increase of signal-to-noise ratio. Using this cryoprobe it is even possible to perform ^{13}C NMR analyses on a small quantity of a material with a reasonable acquisition time for sample concentrations as low as 0.9–3.2 mg/mL. These concentrations are significantly lower than the concentrations usually used in ^{13}C NMR with a conventional probe [131, 132]. Cong et al. [133] used this cryoprobe and collected fractions from 20 chromatographic runs. After evaporation of the mobile

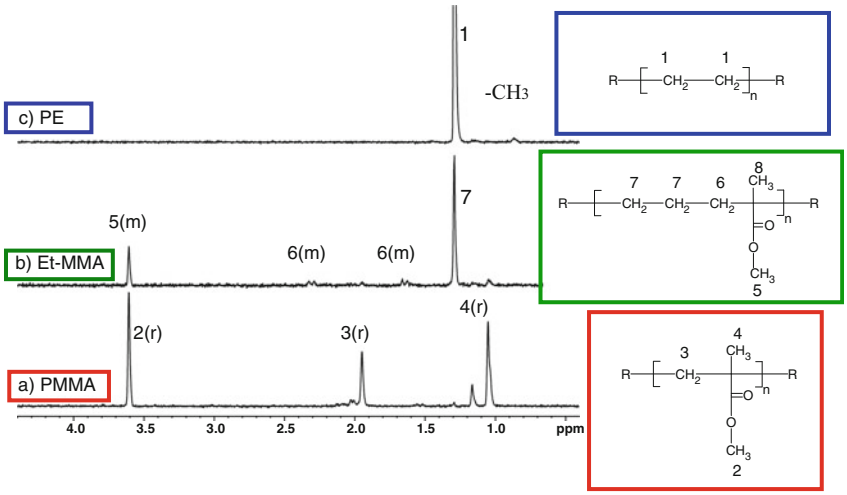

Fig. 17 ^{1}H traces of the on-flow run of Fig. 16: (**a**) PMMA (RT = 60.5 min); (**b**) PE–PMMA copolymer (RT = 66.0 min); (**c**) PE 1,100 g/mol (RT = 79.4 min)

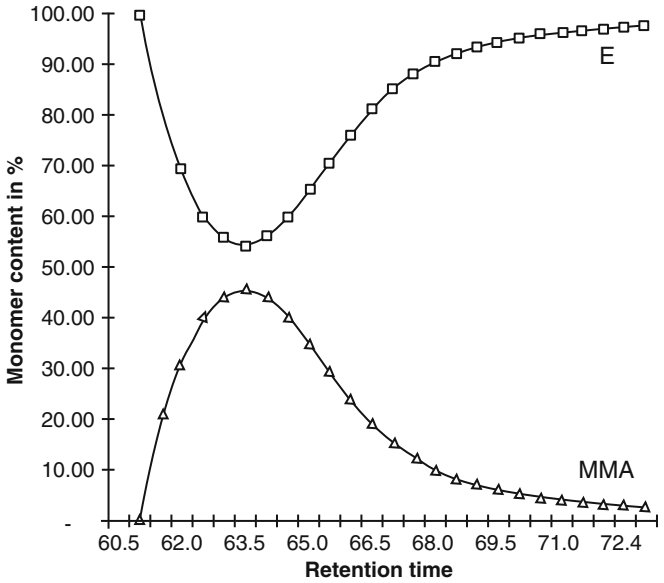

Fig. 18 Monomer composition of PE–PMMA copolymer vs. retention time

phase NMR measurements were performed. The new cryoprobe enabled one to determine the content of octene in the collected copolymer fractions, thus demonstrating the practical applicability of the excellent improvement of detectability of polyolefins in NMR.

3.2 Interaction Chromatography

As described in the previous sections, there are a number of fractionation techniques that are used very successfully in polyolefin analysis, including HT-SEC, CRYSTAF and TREF. For copolymers, CRYSTAF and TREF provide information about the chemical composition distribution. The drawbacks of these methods are that (1) they are very time-consuming and (2) they work only for crystallizable polyolefins. The latest development in this field, CEF, is able to obtain similar results to TREF in less than 1 h and is, therefore, a significant improvement. Still, CEF is based on crystallization and can only address the crystallizable part of a polyolefin sample.

On the other hand, high-performance liquid chromatography (HPLC) is an important tool for the fast separation of complex polymers with regard to chemical composition. HPLC separations can be achieved via different mechanisms, including adsorption–desorption and precipitation–redissolution. In gradient HPLC, precipitation and adsorption processes are frequently combined.

Until recently, standard HPLC methods for polymers, e.g., gradient chromatography or chromatography at critical conditions (LCCC), were limited to ambient or slightly elevated temperatures [134, 135]. The majority of published HPLC separations were conducted at operating temperatures of a maximum of 80°C. These temperatures are too low for the dissolution of polyolefins, which require at least 120°C for dissolution due to their mostly semicrystalline nature. It was, therefore, a challenge to develop HPLC methods for the separation of polyolefins that operate at temperatures of 120°C and higher.

The first attempts to use interactive stationary phases for the separation of polyolefins started in 2003. Macko et al. used an isocratic separation system for PE–PP blends [136, 137]. For the separation of the two polymers, TCB was used as a thermodynamically good solvent for both components and ethylene glycol monobutylether (EGMBE) as eluent. Dimethylsiloxane-modified silica gel was used as stationary phase. As a result, PE eluted almost irrespective of its molar mass under limiting conditions, while PP eluted in the SEC mode before the PE components. Resolution of this method, however, was rather poor and additionally limited by the poor solubility of the polyolefins. These results triggered some in-depth studies on the solubility of polyolefins in different solvents using cloud point titration [138] and the testing of zeolites as selective stationary phases [139–142].

It was found that PE can be adsorbed on specific zeolites from some polar non-solvents as well as from good solvents, such as decalin or TCB which are typically used for SEC of polyolefins. Full or partial adsorption of PE and isotactic PP on different column packings were found; see a summary in Table 4 [143]. The pores of some zeolites, e.g., SH-300, correspond to the diameter of PE in its linear conformation but are smaller than the corresponding diameter of PP. Thus, PE but not PP may be adsorbed into the zeolite SH-300 from a specific solvent, see Table 4. The adsorption of PP requires a zeolite with larger pore diameter, e.g., zeolite CBV-700. NMR measurements confirmed the penetration of PE into the

pores of zeolites SH-300 and CBV-780 [142]. The adsorption isotherms for PE in TCB/zeolite were experimentally measured [144]. Conditions to desorb the retained polymers from the zeolites were, however, not found. Still, the different retention behaviour of PE and PP in some solvent/zeolite pairs enabled selective removal of PE or isotactic PP from mixtures of both [145].

Pronounced retention of PE and PP on silica gel and other macroporous sorbents (see Table 4) were found using solvents such as tetrachloroethane or trichloropropane as mobile phases [146]. Unfortunately, these solvents partially chlorinate PE, cause corrosion of metallic components in the chromatograph and are, thus, not suitable for practical use.

3.2.1 HT-HPLC Instrumental Background

The separation of complex polymers by interaction chromatography most frequently requires an instrument that has the flexibility to conduct isocratic and solvent gradient separations. In particular for high molar mass polymers, gradient elution is unavoidable to ensure complete elution and full recovery. For polyolefin analysis such an instrument must be capable of handling solvent mixtures and gradients at high temperatures. In 2004, as a joint development of Polymer Laboratories, Ltd. (Church Stretton, England) and the group of Pasch and Macko, the first instrument that combines both high operation temperatures and the necessary requirements for gradient HPLC was introduced [147]. This (first of its kind) pioneering instrument contained a high pressure gradient pump for either running a binary solvent gradient or pumping a single solvent (SEC) or a mixture of two solvents at constant composition (for HPLC); see Fig. 19.

Mobile phase changes were accomplished via a multi-solvent management system. The chromatograph was equipped with a robotic sample handling system, which enabled sample preparation and injection at temperatures up to 220°C. For fast column and mobile phase screening, a column switching valve inside the column compartment enabled the successive use of up to six different columns (or five columns and a reference capillary for direct injection into the detector). The choice of detectors for high-temperature HPLC of polyolefins and their copolymers is very limited. The present instrument contained a high-temperature differential refractive index (RI) detector for isocratic elution (e.g., SEC and LCCC) and an ELSD for gradient and isocratic elution modes. The ELSD was attached to the chromatograph via a heated transfer line.

3.2.2 HT-HPLC at Critical Conditions

At critical conditions, polymers of identical chemical composition elute at the same elution volume irrespective of their molar masses. Examples of such chromatographic behaviour were published in 2003 for more than 150 sorbent–eluent systems [148]. However, in nearly all cases the critical conditions were obtained

Table 4 Overview of elution behaviour of isotactic PP and linear PE on different column packings. (Reprinted from [143] with permission of Wiley-VCH)

Solvent ↓	Microporous sorbents (zeolites)									
	SH-300 Si/Al = 150 Pores 5–6 Å		Silicalite Si/Al = 400 Pores 5–6 Å		CBV-780 Si/Al = 40 Pores 7–12 Å Mesopores 40–400 Å		CP814E β Si/Al = 12.5 Pores 5.6–7.5 Å		MCM-41 Pores 44 Å	
Polymer →	PP	PE	PP	PE	PP	PE	PP	PE	PP	PE
TCB	E	**PR**	E	E	E	E	E	**FR**	E	E
Decalin	E	**FR**	E	**PR**	E	**PR**	E	**FR**	E	E
Tetralin	E	**PR**	E	E	E	E	E	**FR**	E	E
1,4-Dimethylbenzene[a]	E	**FR**	E	E	E	E	E	**FR**		
1,2-Dichlorbenzene	E	**FR**	E	E	E	E	E	**FR**		
1,3-Dichlorobenzene	E	**PR**	E	E	E	E	E	**FR**		
1,3,5-Trimethylbenzene	E	**FR**	E	**PR**	E	E	E	**FR**	E	E
1,1,2,2-Tetrachlorethane[a]	E	**FR**	E	E	E	E	E	**FR**	E	E
Tetrachlorethylene[b]	E	**FR**	E	E	E	E	E	**FR**		
Diphenylether	E	**FR**	E	E	**FR**	E	E	**FR**	E	E
Cyclohexanol					**PR**	**PR**				
n-Decanol	E	E	E	E	**PR**	**PR**	E	E	E	E
n-Dodecanol					**PR**	**PR**				
Diphenylmethane					**PR**	**PR**				

Solvent ↓	Macroporous sorbents									
	Silica gel Pore size 100 Å		Aluminium oxide Pore size 200 Å		Zirconium oxide Pore size 150 Å		Hydroxy-apatite Pore size 300 Å		Florisil Pore size 300 Å	
Polymer →	PP	PE	PP	PE	PP	PE	PP	PE	PP	PE
1,12,2-Tetrachloroethane	**PR**	**PR**	**PR**	**FR**	**PR**	**PR**	**PR**	**FR**	**PR**	**PR**
1,2,3-Trichloropropane	**PR**	**PR**	**PR**	**PR**	**PR**	**PR**	**PR**	**PR**	**PR**	**PR**
1,1,2,2-Tetrachloroethylene	E	E	E	E	E	E	E	E	E	E

[a]Measured at 110°C

[b]Measured at 135°C. Other data measured at 140°C

FR full retention of polymers on sorbent, **PR** partial retention of polymers on sorbent, *E* full elution of polymers from sorbent

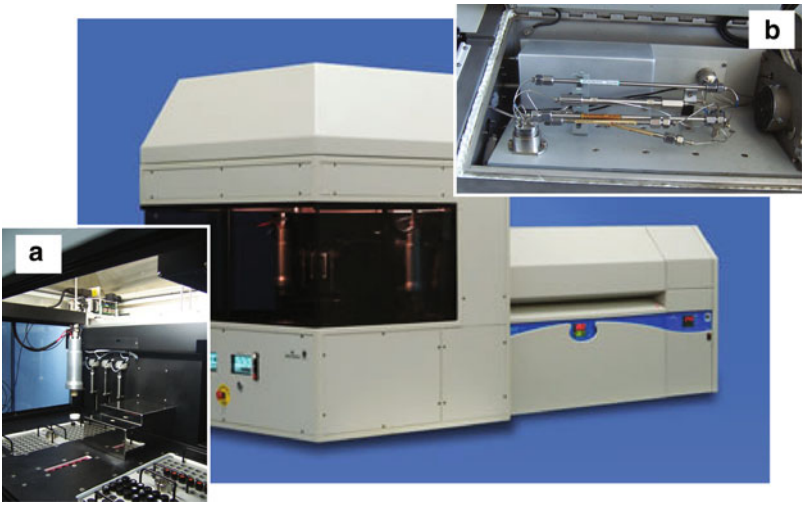

Fig. 19 Polymer Labs HT-HPLC instrument with sample robot (**a**) and column switching valve (**b**)

only for applications operating at ambient temperature. Chromatographic separations of polyolefin blends and copolymers, however, must be carried out at temperatures >100°C to ensure that the samples are completely dissolved.

The analysis of polyethylene–polystyrene blends by LCCC is presented in Figs. 20 and 21. With polar Lichrosorb as the stationary phase and decaline–cyclohexane as the mobile phase, using a column temperature of 140°C, blend separations can be accomplished. The adjustment of the critical mobile phase composition is shown in Fig. 20. As can be seen, the elution behaviour of polystyrene changes appreciably even with changes of the mobile phase composition by only 0.1 vol% [149]. This demonstrates the importance of high accuracy and reproducibility of the mixing of desired mobile phase compositions. The critical mobile phase composition corresponds to decaline-cyclohexane 95.9:4.1% by volume, indicated by the molar mass independence of the elution volume.

Figure 21 illustrates the separation of polystyrene–polyethylene blends at LCCC conditions. As can be seen, polyethylene elutes in the SEC mode whereas polystyrene elutes irrespective of its molar mass. The full separation of the blend components is accomplished within only 4 min. In addition to the separation of blends, the critical conditions for polystyrene were used for the separation of polystyrene/polyethylene block copolymers.

Critical conditions for polymethyl methacrylate at a temperature of 140°C have also been identified. The separation of ethylene/methyl methacrylate block copolymers with high-temperature LCCC is described in [150].

The critical conditions for PE or PP have not yet been experimentally demonstrated in such a typical way. The identification of the corresponding critical conditions could, however, enable one to determine MMD of each block in diblock copolymers similar to what has been shown several times for ambient temperature.

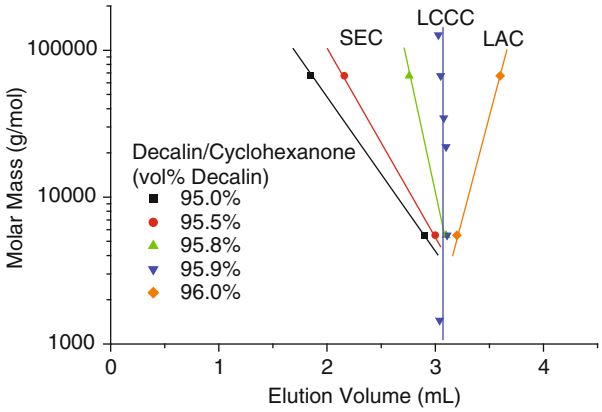

Fig. 20 Dependence of the elution volume of polystyrene standards on the composition of the mobile phase. Mobile phase: decalin-cyclohexanone (in vol.%). Column: Lichrosorb 100, 250 mm × 4.6 mm I.D. Temperature: 140°C. Detector: PL-ELS 1000. Flow rate: 1 mL/min. (Reprinted from [149] with permission of Taylor & Francis)

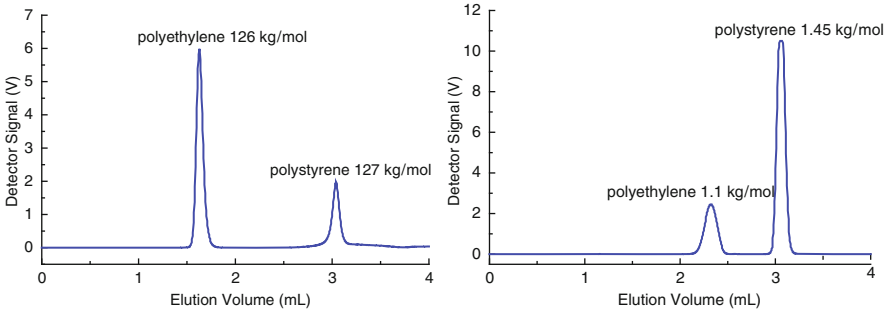

Fig. 21 Chromatograms of blends of polyethylene and polystyrene with similar molar masses obtained at LCCC conditions for polystyrene. Mobile phase and sample solvent: decalin-cyclohexanone 95.9:4.1 vol.%. Other experimental conditions see Fig. 20. (Reprinted from [149] with permission of Taylor & Francis)

Macromolecules with different endgroups or macromolecules which differ in their topological structure (for example, linear contra cyclic) could also be selectively separated under the critical conditions.

3.2.3 HT-HPLC Based on Precipitation-Redissolution

Various combinations of solvents and non-solvents were tested for preparative separations of polyolefins according to their molar masses and/or chemical compositions. Lehtinen et al. [151] used ethyleneglycol monobutyl ether (EGMBE) for the preparative separation of polyolefins using the fact that EGMBE is a good

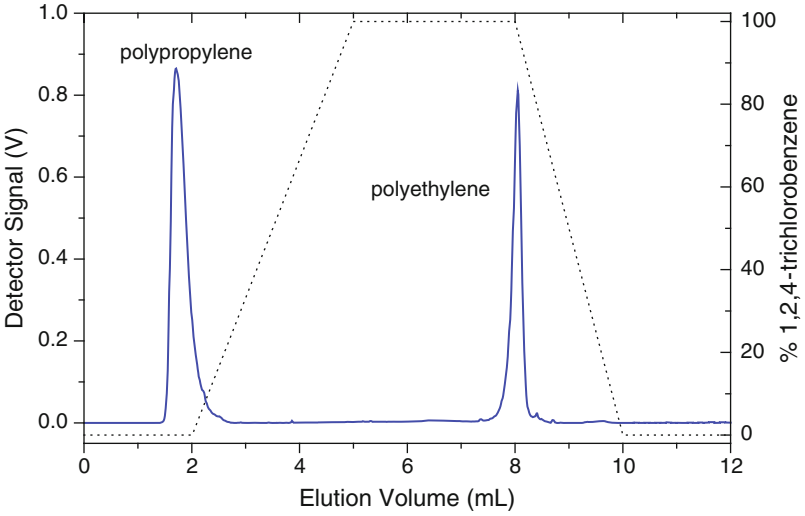

Fig. 22 Chromatogram of a blend of isotactic polypropylene (305 kg/mol) and linear polyethylene (126 kg/mol). Stationary phase: Nucleosil 500, 250 mm × 4.6 mm I.D. Mobile phase: gradient of EGMBE and TCB (*dotted line*); temperature: 140°C; detector: PL-ELS 1000; sample solvent: *n*-decanol; injection volume: 50 µL; concentration: 1 mg/mL. (Reprinted from [152] with permission of Elsevier Limited)

solvent for polypropylene but a non-solvent for polyethylene. It has been shown now that EGMBE as the mobile phase and an oligo(dimethyl)siloxane modified silica gel as the stationary phase enable HPLC separation of polyethylene from polypropylene. As the injection solvent in this case TCB is used [136]. In this system PP eluted in the size exclusion mode whereas PE eluted with the solvent peak at limiting conditions. However, there was a serious problem with regard to full recovery of polyethylenes with higher molar masses. In addition, the resolution of the separation method was limited.

With the PL XT-220 gradient system it became possible to overcome these limitations. With a solvent gradient of a good solvent for both polyethylene and polypropylene, full recovery of the sample was achieved. Using a weaker sample solvent, the elution of PE with the sample solvent was suppressed. If the sample was dissolved in *n*-decanol instead of TCB and a gradient EGMBE–TCB was applied to a silica gel column, a baseline separation of PE and PP was achieved, as illustrated in Fig. 22 [152]. In this case PE was completely precipitated on the column with the initial mobile phase, while PP eluted in the size exclusion mode. When the content of TCB in the mobile phase was increased by performing a gradient the precipitated polyethylene was eluted.

As was shown, for the first time blends of different polyolefins were separated quantitatively over a wide range of concentrations by liquid chromatography at 140°C. Moreover, EPC were separated into a propylene-rich part and an ethylene-rich part [153]. This chromatographic approach was also applied to the separation of EPC [55]

and for the separation of various polyolefins with regard to the chemical composition of the components [154].

3.2.4 HT-HPLC Based on Adsorption–Desorption

Functionalized Polyolefins

As one very striking example of the capabilities of the high-temperature gradient HPLC system, the separation of random ethylene/vinyl acetate copolymers is presented in Fig. 23. On silica gel as the stationary phase and using decaline–cyclohexanone as the eluent, full separation of copolymers of different compositions was achieved. In addition, the homopolymers PE and PVAc were well separated from the copolymers. This was the first time that a chromatographic system was available that separates olefin copolymers irrespective of crystallinity and solubility over the entire range of compositions. Namely, the mobile phase components used are solvents for both PE and PVAc. The non-polar solvent, decalin, supports adsorption of PVAc on the silica gel, while the polar solvent, cyclohexanone, enables desorption and elution of the adsorbed polymer sample from the column [155].

In a next step, this highly selective type of copolymer separation was coupled to FTIR spectroscopy to analyze the CCD of the samples. For the HPLC-FTIR coupling the LC Transform interface system was used; see Fig. 24. The results of the FTIR coupling are presented in Fig. 25 for three EVA copolymer samples.

Figure 25 shows the elugrams of the samples presented as Gram–Schmidt plots. The Gram–Schmidt plots are obtained from FTIR measurements by summarizing all peak intensities at all frequencies and compare well with the total concentration profile. Across the Gram–Schmidt plots the vinyl acetate (VA) contents are given as

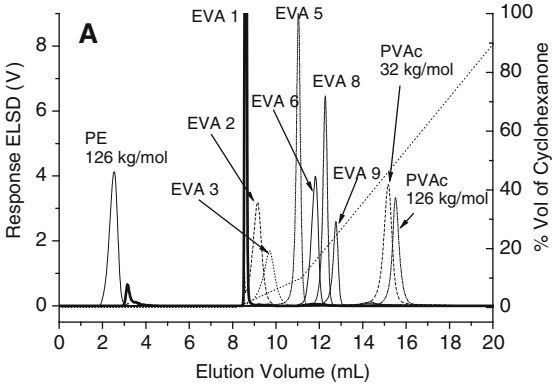

Sample	M_w [kg/mol]	VA [wt.%]
EVA 1	330	5
EVA 2	270	12
EVA 3	330	14
EVA 5	144	28
EVA 6	430	45
EVA 8	370	60
EVA 9	267	70

Fig. 23 Overlay of the chromatograms of EVA copolymers; stationary phase: Polygosil 1000; mobile phase: gradient decalin/cyclohexanone (*dotted line*); temperature: 140°C; detector: ELSD; sample solvent: decalin (TCB for the PVAc standards). (Reprinted from [155] with permission of American Chemical Society)

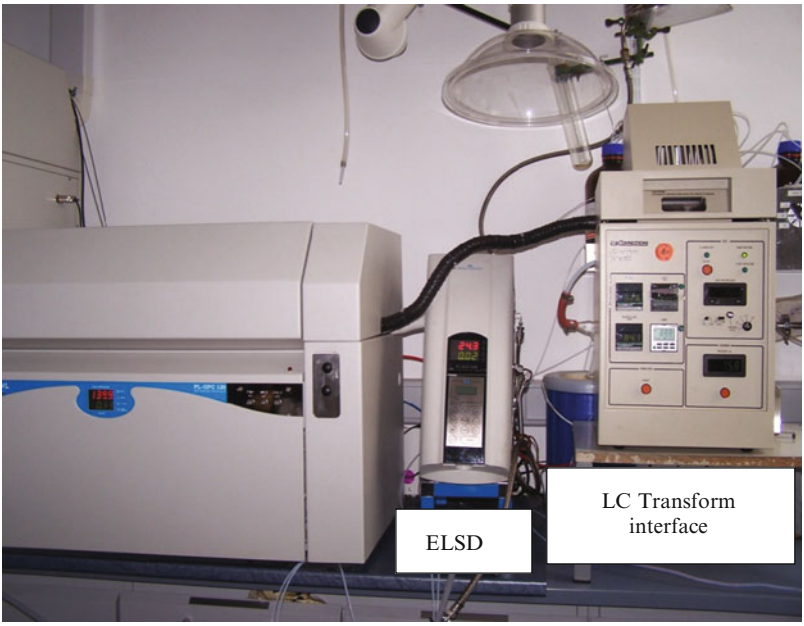

Fig. 24 Coupling of the HT-HPLC system to the ELSD for concentration detection and the LC Transform interface. (Reprinted from [156] with permission of Wiley-VCH)

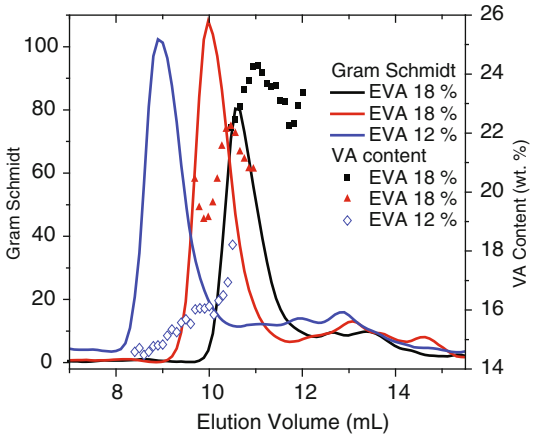

Fig. 25 Separation of three EVA samples with regard to chemical composition, the vinyl acetate contents across the elution curves are presented as *dotted lines*. (Reprinted from [156] with permission of Wiley-VCH)

obtained from the ratio of the peak for the carbonyl group (1,736 cm^{-1}) to the peak of the CH_2 vibration (1,463 cm^{-1}, presenting the total polymer concentration). This peak ratio is correlated with true copolymer compositions that were obtained

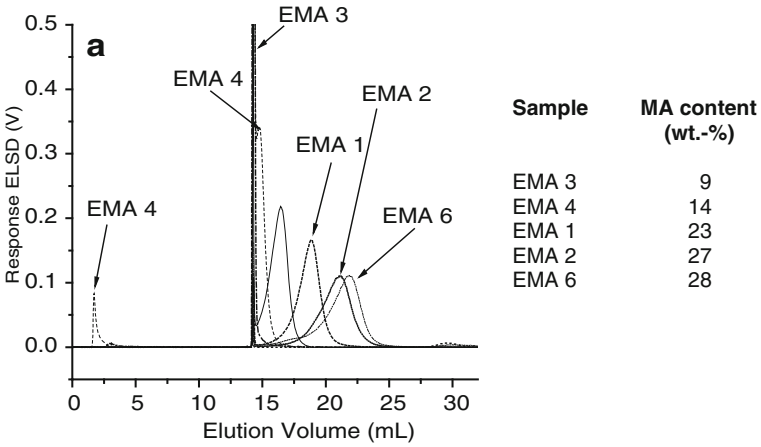

Fig. 26 Overlay of the chromatograms of ethylene-methyl acrylate (EMA) copolymers; stationary phase: Perfectsil 300; mobile phase: gradient decalin/cyclohexanone; temperature: 140°C; detector: ELSD; sample solvent: decalin. (Reprinted from [118] with permission of Wiley-VCH)

by NMR. As can be seen there is a clear correlation between the VA content and the elution volume, indicating that, indeed, separation takes place with regard to the chemical composition of the copolymer. It is interesting to see that the two samples with the same nominal VA content (18%, curves, triangles and squares) show distinctively different elution patterns. This clearly demonstrates that HPLC-FTIR provides very detailed structural information.

In a similar approach, ethylene/acrylate copolymers were analyzed. Figure 26 shows the separation of ethylene/methyl acrylate copolymers by high-temperature gradient HPLC. In this case a silica gel Perfectsil 300 was used as the stationary phase. The mobile phase was a gradient of decaline–cyclohexanone [118].

The advantage of the above separation systems is that not only the copolymers are separated according to their composition but also the corresponding homopolymers elute at just opposite positions: PE first as a non-retained sample and PVAc, PBA, PMA or PMMA as the last eluting sample in the chromatogram.

Polyolefins

Considering the fact that adsorption of polyolefins was found on zeolites, further research was conducted to find systems where both adsorption and desorption take place under conditions that are compatible with chromatographic experiments. In a ground-breaking study Macko and Pasch found that a specific carbon based stationary phase – Hypercarb (http://www.interscience.be/promotiesites/hypersil/topics/promotiesites/hypersil/nieuws/hypercarb_technical.pdf) – enables highly selective separations of polyolefins. Hypercarb was originally developed by Knox and coworkers [157] and had been used in HPLC analysis of small molecules; it

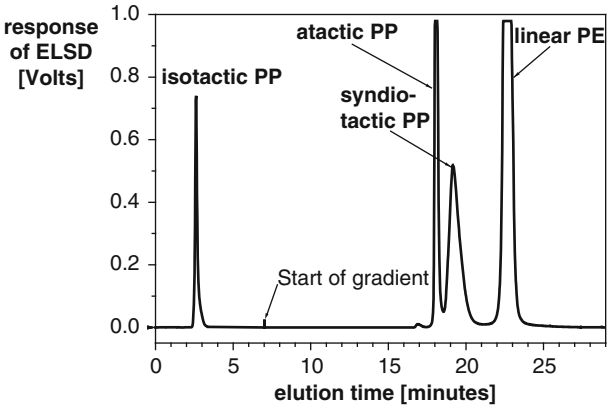

Fig. 27 Separation of a blend of isotactic, syndiotactic and atactic PP and linear PE; stationary phase: Hypercarb; mobile phase: gradient 1-decanol/TCB; temperature: 160°C; detector: ELSD. (Reprinted from [159] with permission of American Chemical Society)

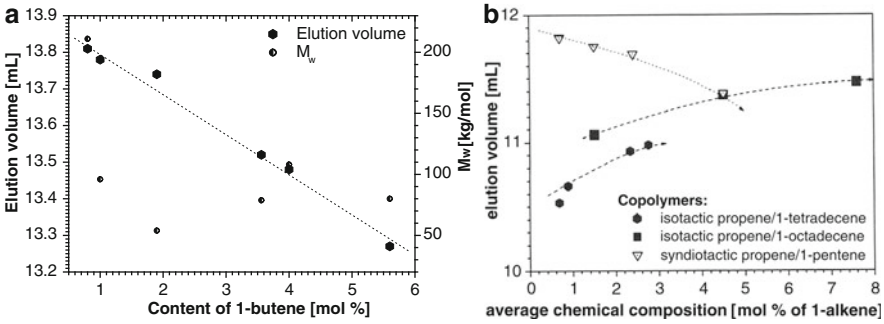

Fig. 28 Dependence of elution volume on average chemical composition of copolymers, (**a**) ethylene-1-butene copolymers, (**b**) propylene-1-alkene copolymers; stationary phase: Hypercarb; mobile phase: gradient 1-decanol/TCB; temperature: 160°C; detector: ELSD. (Reprinted from [161] and [162] with permission of Springer Science + Business Media and Elsevier Limited)

was, however, never applied to separate synthetic polymers. Macko et al. found that porous carbon Hypercarb adsorbs linear PE from 1-decanol as the mobile phase at 160°C [158–160]. The retained polymer was desorbed from the column using a linear gradient from 1-decanol to TCB. Moreover, this HPLC system separated isotactic, atactic and syndiotactic PP from each other (Fig. 27). It was shown further that the same chromatographic system separates ethylene–hexene and propene/1-alkene copolymers according to their chemical compositions (Fig. 28) [162, 163]. It turned out that the elution volumes of the ethylene/1-butene and ethylene/1-hexene copolymers depend linearly on the average chemical composition (Fig. 28a), with an increase in the content of ethylene resulting in an increase in the retention volumes. This behaviour could be traced to a stronger

adsorption of PE on the graphite surface as compared to other polyolefins. It was supposed that PE is adsorbed on the planar surface of graphite in a monomolecular layer with its molecular axis lying parallel to the graphite surface, forming a closely packed layer. The introduction of short branches (e.g., ethyl or butyl branches in 1-butene or 1-hexene) sterically hinders the formation of closely packed layers on the graphite surface, thus acting against adsorption. Therefore, the introduction of 1-butene or 1-hexene leads to a decrease in the retention volume of the ethylene/1-alkene copolymers (Fig. 28a). Isotactic PP chains or iPP blocks do not adsorb on graphite surface from 1-decanol [158–160]. The introduction of adsorbing 1-alkene groups (i.e., branches containing more that 11 carbons) leads to an increase in the retention volumes of the propene/1-alkene copolymers (Fig. 28b). The elution behaviour of syndiotactic PP/1-pentene copolymers follows the same trend as that of the ethylene/1-alkene copolymers, because sPP blocks are adsorbed and the introduction of short branches acts against adsorption.

The major achievement of this adsorption based HPLC system is that it can be used to analyze semi-crystalline as well as amorphous polyolefin samples, which is a significant step forward from the previously known methods since TREF and CRYSTAF can only be applied to semi-crystalline samples. Macko et al. demonstrated the usefulness of the approach for EPC [164] and copolymers of propylene with different tacticities [165]. Moreover, terpolymers of ethylene, propylene and a diene monomer (EPDM) were separated [166]. It was found that both comonomers, ethylene and diene, are adsorbed. On the other hand, adsorption of EP [164], ethylene-butene (EB), ethylene-hexene (EH), ethylene-octene (EO) or ethylene/1-decene copolymers depends linearly on the average content of ethylene [161]. This is very practical from the point of evaluation of chromatograms. Such linear dependence enables one to calibrate the elution volumes in order to estimate the chemical composition of a sample directly from its position on a chromatogram. The peak height which reflects the concentration of the sample must be calibrated if precise concentrations of the separated components are required. Moreover, the choice of suitable solvents and temperatures enables one to separate these copolymers in the range of 0–100% of a corresponding monomer. For example, EO copolymers can be separated in the system 1-decanol/TCB/Hypercarb only in the range of 0–60 mol% of octene at a temperature of 175°C [167], while using a temperature of 140°C enabled the separation of EO copolymers in the range of 0–100% in the system 1-decanol/TCB/Hypercarb [168]. Such separation of EO copolymers can also be realized at a temperature of 160°C if, instead of 1-decanol as the mobile phase, 2-octanol is used [169].

Experiments confirmed that the molar mass or long chain branching in the above-mentioned samples [166] does not influence the HPLC separation. Independence of the elution volumes on the molar mass >15–20 kg/mol was also found for PE [164] and EP, EB, EO and ethylene/1-decene copolymers [161]. It is typical for adsorption phenomena that adsorption depends on the shape of a molecule, on positions and numbers of functional groups, on polarizability of the molecule, as well as on the type and nature of the sorbent and the solvents. Fine tuning of the adsorptive interactions enables one to reach extremely sensitive and specific chromatographic separations. This represents an additional advantage of HPLC in

comparison with conventional methods such as TREF. It makes it possible to separate polyolefins according to specific details in their chemical composition, something that was never realized in the past.

3.3 *Temperature Gradient Interaction Chromatography*

It is known that adsorption of polymers is a function of temperature [170]. This phenomenon has been applied to the separation of synthetic polymers by Lochmüller [171] for poly(ethylene glycol) and by Chang [172] for polystyrene. Very recently, Cong et al. described experimental conditions which enable one to apply temperature changes to the separation of polyolefins [133]. Separation was achieved by the interaction of the polyolefin with a graphite surface in a thermodynamically good solvent for PE. The solvent was *o*-dichlorobenzene and the commercially available Hypercarb column was used.

The ethylene/octene copolymers were dissolved in ODCB and injected into the column flushed with the solvent. After injection, a temperature gradient was applied; see Fig. 29 and the definition of the experimental variables in Table 5. As a consequence, the samples eluted from the column in an elution order illustrated in Fig. 30. PE eluted at 150°C. This temperature is about 49°C higher that the peak elution temperature in TREF and CEF and ~15°C higher than the peak melting temperature of DSC. This demonstrates the strong attractive interactions between the graphite surface and PE. TGIC was therefore capable of analyzing samples with comonomer contents of 0–50 mol%, which exceeds the range 0–9 mol%, which was achieved for this type of samples with the conventional

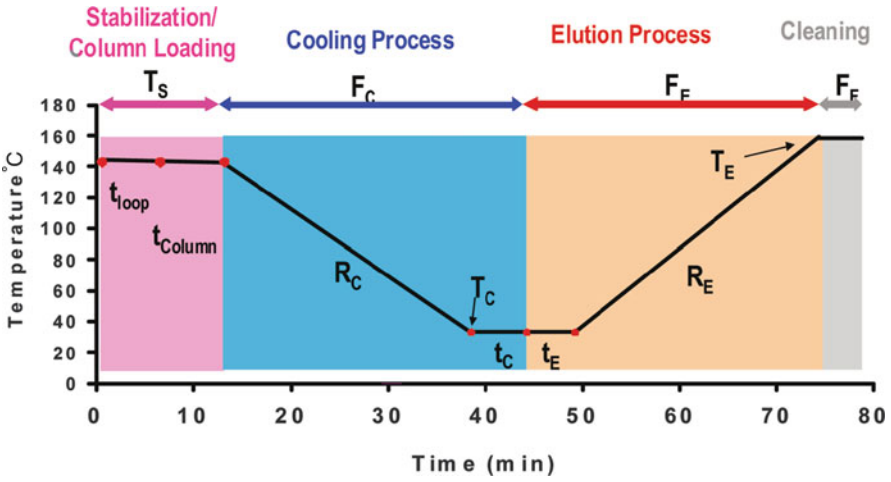

Fig. 29 Schematic of HT-TGIC experimental setup, the definition of each variable is described in Table 5. (Reprinted from [133] with permission of American Chemical Society)

Table 5 Definition of the experimental variables for TGIC. (Adapted from [133] with permission of American Chemical Society)

Variable	Symbol	Description
Stabilization and sample loading process		
Stabilization rate (°C/min)	R_S	Thermal rate for the temperature changing from the dissolution temperature to the stabilization temperature
Stabilization temperature (°C)	T_S	Temperature during stabilization and at the start of cooling process
Stabilization time (min)	t_{LOOP}	Amount of time the sample stays in the injection loop in the top oven of CEF before being loaded into the column
Precooling time (min)	t_{COLUMN}	Amount of time the sample stays in the front of the column before cooling process begins
Cooling process		
Cooling rate (°C/min)	R_C	Thermal rate of the main oven (where TGIC column is located) during cooling process
Final temp of cooling process (°C)	T_C	Final temperature at the end of cooling process
Postcooling time	t_C	Time that the sample stays in the column at the final temperature of cooling process; pump flow rate of cooling process continues but data is not collected
Flow rate of pump during cooling process (mL/min)	F_C	Flow rate during cooling process; it can be zero (static cooling process) or nonzero (dynamic cooling process)
Elution process		
Elution rate (°C/min)	R_E	Thermal rate of the main oven (where TGIC column is located) during elution process
Final temperature of elution process (°C)	T_E	Final temperature at the end of elution
Soluble fraction time	t_E	Amount of time that the main oven stays of the final temperature of cooling process while pump being at flow rate of elution process before increasing temperature; data collection begins here; the purpose is to have a well separate SF peak in chromatogram
Flow rate of pump during elution process (mL/min)	F_E	Flow rate during elution process

crystallization based techniques. The authors claim that co-crystallization does not play a role in TGIC. Moreover, they emphasize that TGIC, in contrast to HT-HPLC, uses a single solvent as the mobile phase, enabling one to detect the polymers with different detectors, including a light scattering detector, refractometer, infrared or viscosimetric detector. This is true for HT-TGIC as well as for HT 2D-LC, which will be discussed in the next section.

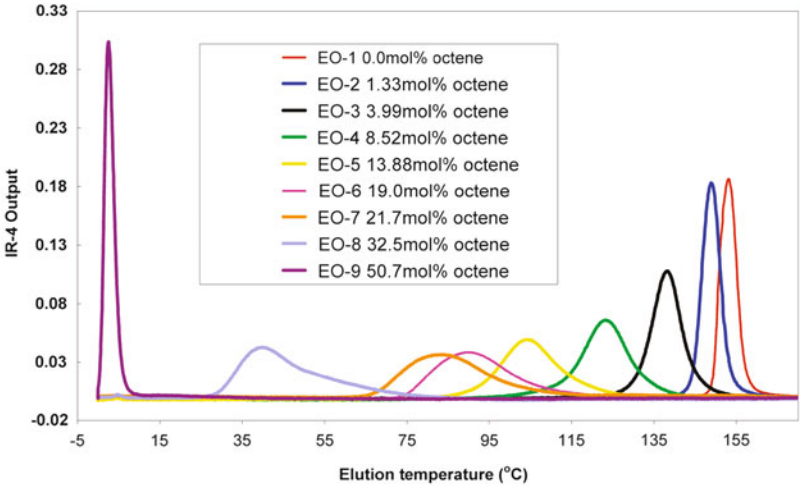

Fig. 30 TGIC chromatograms of EO-1 to EO-9, HYPERCARB column, the TGIC experimental conditions (stabilization temperature 140°C; final temperature during cooling process 0°C; final temperature during elution process 175°C; cooling rate during cooling process 6°C/min; heating rate during elution process 3°C/min; flow rate during cooling process 0.03 mL/min; flow rate during elution process 0.5 mL/min. (Reprinted from [133] with permission of American Chemical Society)

3.4 Two-Dimensional Liquid Chromatography

Coupling of different chromatographic separation methods enables one to resolve multiple distinctive components. Two-dimensional liquid chromatography (2D-LC) has been shown to be an extremely useful tool for the investigation of the molecular heterogeneity of complex polymers [173–176]. Until recently the application of 2D-LC was limited to ambient temperature and it was only in 2010 that the introduction of high-temperature 2D-LC was announced.

The first results on 2D-LC for polyolefins were published by Ginsburg et al. [167, 177] and Roy et al. [178]. Roy et al. [178] applied a separation system that was previously described by Macko et al. [158, 159, 162]. This system was applied to the separation of ethylene/1-octene copolymers regarding chemical composition and molar mass. Ginzburg et al. [177] used an instrument that has recently been developed and commercialized by PolymerChar (Valencia, Spain). They used the on-line coupling of gradient HPLC and SEC to separate blends of PP stereoisomers, ethylene/propylene rubbers, ethylene/norbornene copolymers and ethylene/1-hexene copolymers, all at an operating temperature of 160°C using a stationary phase of Hypercarb and a mobile phase of 1-decanol-TCB.

The 2D contour diagram (composition vs. molar mass) for one example is shown in Fig. 31a. This is a most convincing application that gives a clear idea of the capabilities of HT-2D-LC. In a similar experiment a complex mixture of PE and PPs with different tacticities has been separated; see Fig. 31b.

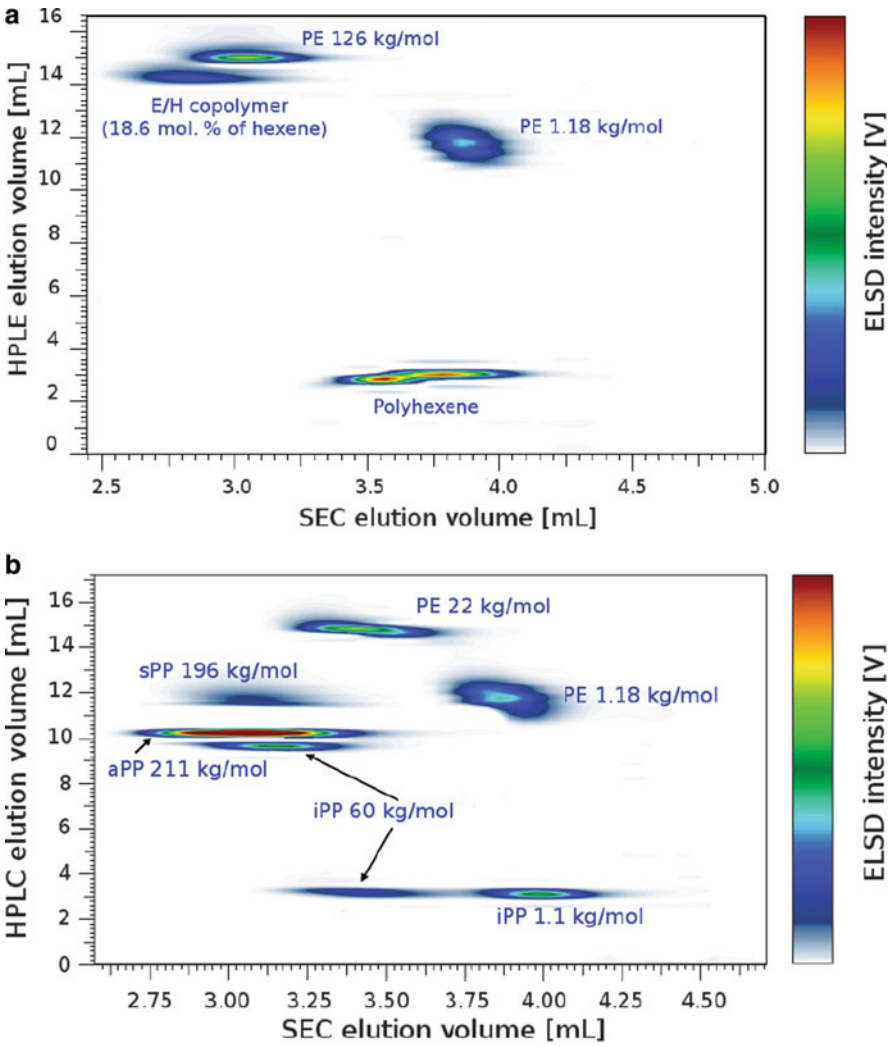

Fig. 31 Contour diagram of the HT-2D-LC separation of (**a**) a blend of PE, poly-1-hexene and an ethylene-1-hexene and (**b**) a blend of PE and PPs with different tacticities; stationary phase: Hypercarb (first dimension) and PL Rapide H (second dimension); mobile phase: gradient 1-decanol/TCB (first dimension) and TCB (second dimension); temperature: 160°C; detector: ELSD. (Reprinted from [167] with permission of Elsevier Limited)

Both axes in a contour plot may be calibrated, as was illustrated very recently for the HT-2D-LC separation of EVA copolymers by Ginzburg et al. [177]. The SEC separation was calibrated with PE standards, while the HPLC separation was calibrated with EVA copolymers with a known content of VA. Moreover, the coupling of HPLC with SEC, where TCB is used as the mobile phase, enables the application of RI, IR, VIS or LS detectors. This was demonstrated recently for

the 2D-LC separation of EP and EO copolymers [179]. Molar masses of the polymers eluting from the 2D-LC system were calculated on the basis of signals from the IR and LS detectors.

The contour plots from 2D-LC differ from those obtained by TREF-SEC because the separation principles are different. While TREF is based on crystallization–dissolution, interactive HPLC is based on the selective adsorption and desorption of the macromolecules. As a result, high-temperature 2D-LC enables selective separation of both semi-crystalline and amorphous polyolefins, whereas TREF-SEC cannot distinguish amorphous components.

4 Field Flow Fractionation

Due to the need for highly detailed information about molar mass, chemical composition, branching and molecular architecture of macromolecular materials, new analytical separation techniques with increased resolution, sensitivity, selectivity and broader applications are constantly sought. Field-flow fractionation (FFF) is a rapidly emerging technique that meets many of these needs. FFF can fractionate a wide range of analytes including macromolecules, colloids and particulates suspended in both aqueous and organic mobile phases [180–183]. It can, therefore, overcome some of the limitations of column based fractionation techniques. As compared to HPLC methods, FFF can fractionate polymers simultaneously regarding molecular size and composition. There is no stationary phase; therefore there are no sample breakthrough effects or sample losses due to adsorption to the stationary phase. The upper limit of FFF extends to the 10^9 Da molar mass range and micron-size particles, thus providing effective separation of microgel components simultaneously with solubilized polymers [184]. In FFF shear degradation is minimized [180, 185–188] which is a significant advantage over SEC for very high molar mass analytes. The mild operation conditions allow the analysis of fragile analytes such as protein aggregates, supramolecular assemblies, and whole cells [182, 189]. Commercial FFF systems have been available since the late 1980s and are currently available from Postnova Analytics, Wyatt Technology, DuPont and ConSenxus.

Medium and high temperature asymmetrical flow FFF (MT-AF4 and HT-AF4) systems have been developed and distributed by Postnova Analytics (Landsberg/Lech, Germany). HT-AF4 has been specifically developed for the separation and characterization of high molar mass polyolefins. Different detectors such as infrared (IR), refractive index (RI), multi-angle light scattering (MALS) and viscometry were applied.

The separation in HT-AF4, which is a specific variation of flow FFF, is provided by a cross-flow perpendicular to the solvent flow as shown in Fig. 32.

The solvent flow passes the empty channel and forms a parabolic velocity profile. The cross-flow leaves through a semi-permeable membrane, which holds the macromolecules back and as a result they are pushed against the membrane.

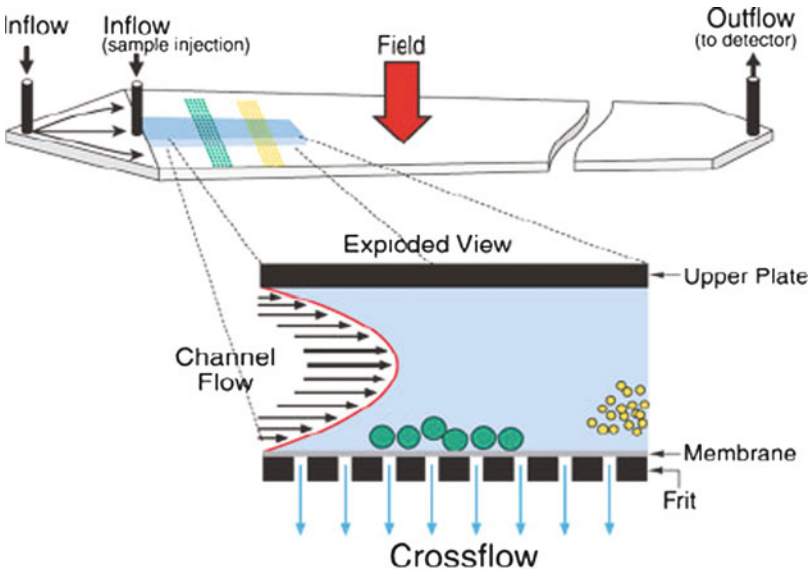

Fig. 32 Cross-section of the AF4 channel, scheme of size separation

The diffusion allows the macromolecules to move back from the accumulation membrane into the channel. As the ability to diffuse depends on molecular size, i.e., small molecules diffuse faster than large molecules, the small molecules will be situated closer to the centre of the profile where the flow velocity is higher. As a result the macromolecules will elute according to their size, beginning with the smallest and fastest moving molecules [185, 190–195].

In HT-AF4, a stainless steel channel and a flexible ceramic accumulation wall membrane is used. This allows measurements with chlorinated organic solvents like TCB at temperatures up to 220°C. The trapezoid channel is cut from a Mylar spacer with a thickness of 250–350 µm. To enhance the performance of the polymer separation a special focusing flow is implemented. This focusing flow is a second input flow, which enters the channel close to the middle and divides itself into two substreams, as shown in Fig. 33. One part of the flow meets the injection flow near the beginning of the channel. Together the two flows form a sharp barrier and leave the channel through the membrane as cross-flow. In the region where both flows come into contact with each other, the sample transported by the injection flow is focused laterally and will rest at the same position until the focus flow stops. The second focus flow substream leaves the channel through the outlet and provides a constant detector flow during the focusing step. This method allows the polymer molecules to be retained at the beginning of the channel after the injection. As a result the molecules can be separated with minimal longitudinal diffusion, which results in less band broadening.

The first AF4 separation at high temperature was done by Giddings et al. [197] for polystyrene. The authors mentioned the possibility to separate PE by HT-AF4

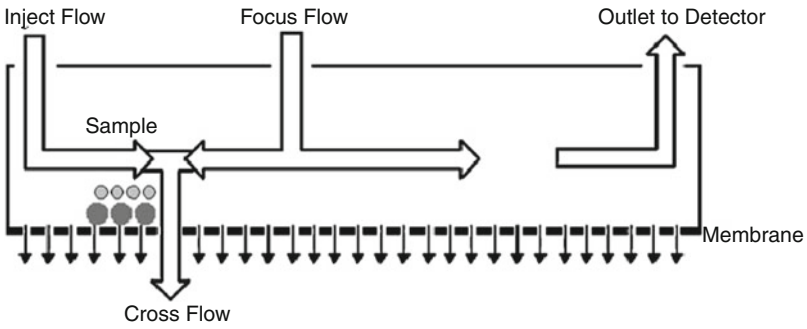

Fig. 33 Flow scheme of the AF4 focussing step. (Reprinted from [196] with permission of Elsevier Limited)

but did not report any results. Several years later, Mes et al. [86] described a first successful separation of polyolefins with HT-AF4. The first commercial instrument for HT-AF4 was developed in cooperation with Postnova Analytics (Landsberg/Lech, Germany) and Polymer Laboratories (Church Stretton, England). Mes et al. used HT-AF4 combined with IR, MALS and viscosity detectors to analyze different samples of high molar mass high density polyethylene (HDPE) and LDPE. The measurements have been compared with the corresponding HT SEC measurements [86]. In the SEC measurements a high molar mass shoulder appeared in the chromatogram for the LDPE samples, which was not observed in the associated fractograms (Fig. 34).The shoulder occurred as a consequence of the low size separation at the exclusion limit of the SEC column. Due to the missing separation of the high molar mass fraction the molar mass average and long chain branching were calculated wrongly as seen by plotting the radius of gyration or the intrinsic viscosity vs. M. Using HT-AF4 molar masses up to 10^8 g/mol could be separated and characterized. In the SEC measurements such molar masses could not be detected due to shear degradation or the size exclusion limit. The presence of shear degradation during the HT-SEC measurements was verified by the comparison with off-line LALS measurements [198].

Another phenomenon, observed in HT-SEC of LDPE, was the abnormal late elution of a small amount of (probably branched) high molar mass material. The co-elution of this fraction with the regularly eluting small molecules was visible as a slight upward curvature in the R_g vs. M plot of LDPE in HT-SEC, as shown in Fig. 35. This result illustrates the numerous advantages of HT-AF4 compared with HT-SEC.

Following the work of Mes et al., a number of detailed studies on the analysis of ultrahigh molar mass polyolefins were conducted by Otte et al. [199–203]. It has been demonstrated that HT-AF4 enables one to separate ultrahigh molar mass samples up to a radius of gyration above 1,000 nm without the disturbing effects typical of SEC, namely the shear-degradation of high molar mass structures and the anomalous late co-elution effects. The problems of erroneous branching calculation and molar mass determination as a result of a curvature in the conformation plot do

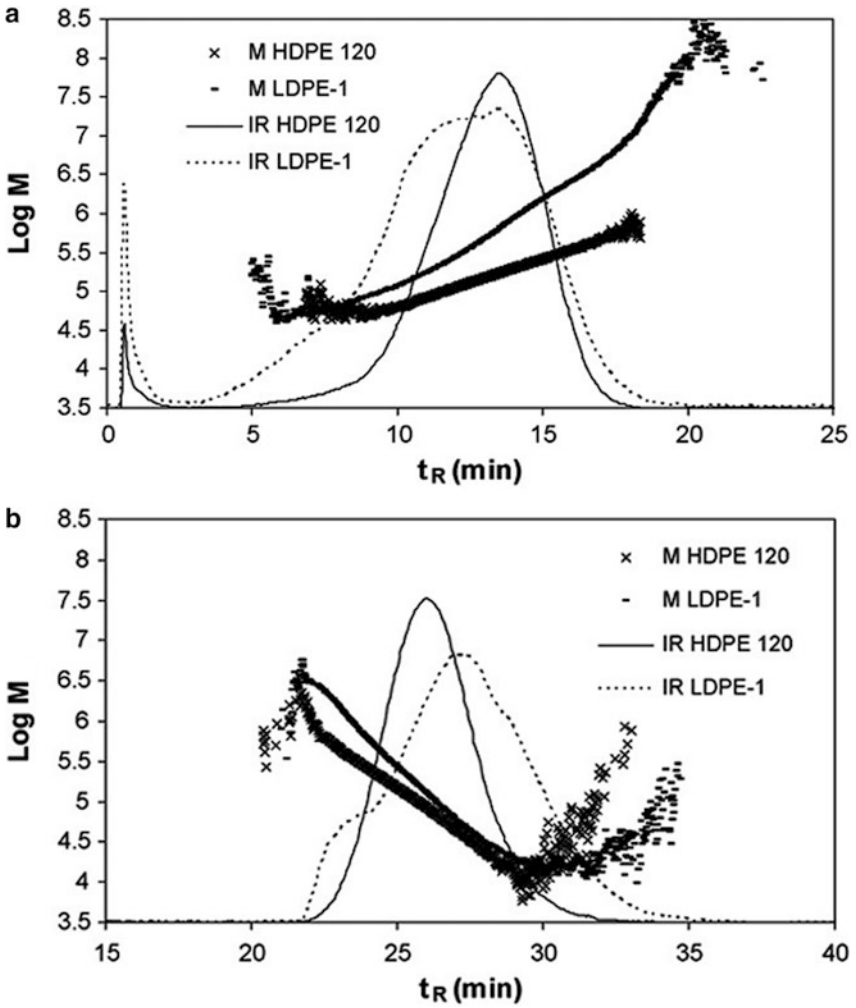

Fig. 34 Elution curves and molar mass plots of LDPE and HDPE samples: (**a**) separation with HT-AF4 and (**b**) separation with HT-SEC. (Reprinted from [86] with permission of Elsevier Limited)

not exist in AF4 and as a result the molar mass averages calculated from HT-AF4 are significantly higher than those obtained from HT-SEC [201].

In a comparative study, linear HDPE has been analyzed by HT-SEC and HT-AF4. The samples had been of low molar mass to minimize shear degradation in HT-SEC. Consequently, both methods provided similar results as can be seen from the conformation plot presented in Fig. 36.

Both graphs are completely congruent and the slope of the R_g–M relationship of 0.6 is very close to the theoretical value of 0.588 for a linear polymer in a good

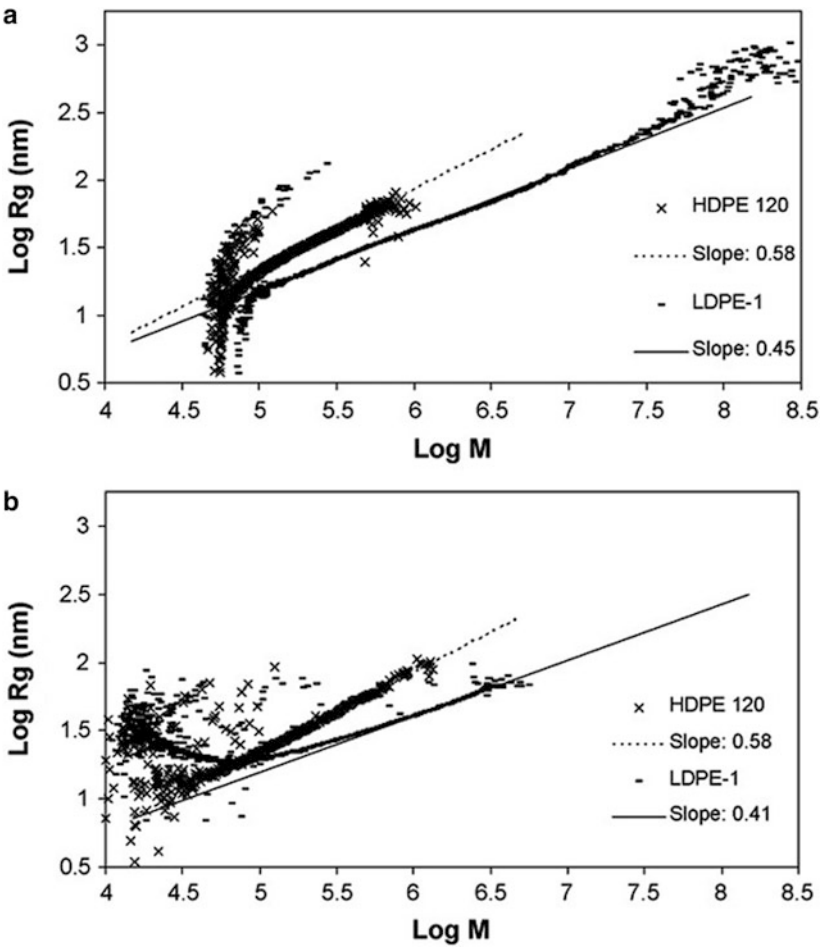

Fig. 35 Comparison of the conformation plots of HDPE and LDPE: (**a**) separation with HT-AF4 and (**b**) separation with HT-SEC. (Reprinted from [86] with permission of Elsevier Limited)

solvent. These results indicate that all system parameters were correctly adjusted and the separation was comparable for both methods.

One problem of HT-AF4 is that macromolecules with a molar mass below 100 kg/mol are not fully recovered due to the relatively high cut-off of the ceramic membrane. This leads to an overestimation of the calculated molar masses for samples which contain such small molecules. The examination of the data below the cut-off mass range, however, has shown that the error of the missing low M_w part is very low compared to the effect of missing shear degradation. At present, novel ceramic membranes with a lower cut-off are under development.

On the other hand, polyolefin samples with very high molar masses and significant branching (UHM-HDPE or LDPE) are often not correctly measured with

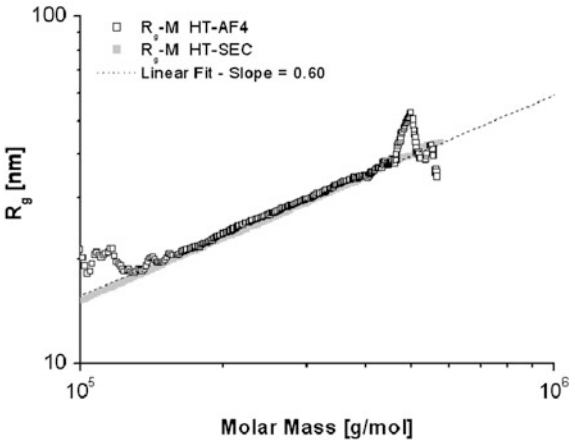

Fig. 36 Conformation plot from HT-SEC and HT-AF4 separation of linear HDPE, data obtained by IR-MALS. (Reprinted from [201] with permission of Elsevier Limited)

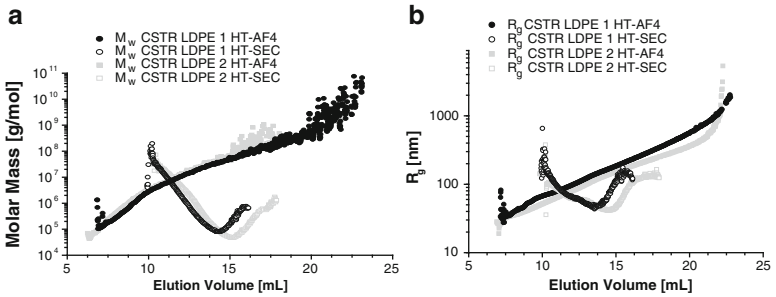

Fig. 37 Overlay of fractograms obtained with HT-AF4 and elugrams from HT-SEC: (**a**) CSTR-LDPE 1 and 2, molar mass obtained by light scattering detection, (**b**) CSTR-LDPE 1 and 2, R_g obtained by light scattering detection. (Adapted from [201] of Elsevier Limited)

HT-SEC due to the abnormal late co-elution of large or branched material which leads to a falsification of the calculated MMD. This has been demonstrated for two ultrahigh molar mass LDPEs that were investigated by HT-SEC and HT-AF4; see Fig. 37. Sample material with molar masses above 1,000 kg/mol is known to be very sensitive to shear degradation in SEC separation. In the case of highly branched material HT-SEC shows abnormal interaction of branched molecules with the stationary phase of the column. As a result the molar mass and the radius of gyration show an abnormal increase at high elution volumes. This effect seems to be caused by the late co-elution of high molar mass molecules together with small linear structures which are eluting according to the regular SEC mechanism.

Figure 37 indicates that the radius of gyration and the molar mass which were detected by HT-AF4 are clearly higher than those detected by HT-SEC. This indicates increased shear degradation in either the packing or the frits of the SEC columns. On the other hand, radii up to 1,000 nm and molar mass values above 10^8 g/mol can be recognized in the HT-AF4 fractograms. For both samples a strong

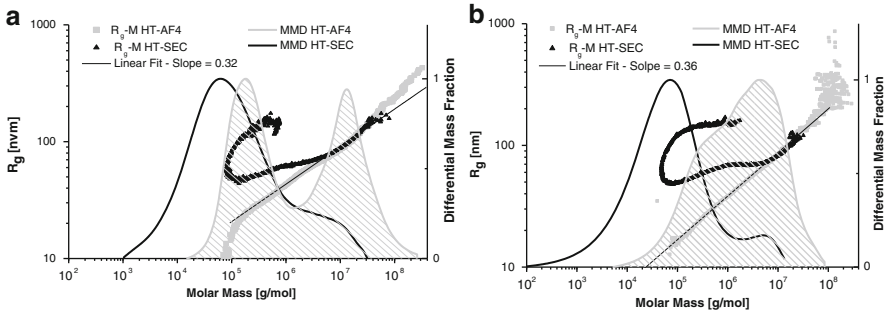

Fig. 38 MMD from HT-AF4 and HT-SEC separation overlaid with corresponding conformation plots obtained by IR-MALS: (**a**) LDPE 1, (**b**) LDPE 2. (Adapted from [201] of Elsevier Limited)

curvature of the radius and the molar mass at high elution volumes is visible in the HT-SEC results. The radius seems to be more affected by the effect which causes the abnormal increase at high elution volumes and co-elution of large and small molecules could be a good explanation for the phenomenon.

HT-AF4 shows no co-elution effect, because no stationary phase is used which could interact with the sample. The molar mass as well as the radius increases steadily with the elution volume. As a result the lower radius values are also visible in HT-AF4 which are not accessible by HT-SEC. In contrast to HT-SEC, HT-AF4 shows a linear dependence between R_g and the elution volume. This indicates a proper separation of the macromolecules according to their hydrodynamic size for the whole sample.

Figure 38 shows the differential MMDs and the conformation plots of both LDPE samples obtained by HT-SEC-IR-MALS as well as HT-AF4-IR-MALS.

The negative effects in HT-SEC manifest themselves in an even more pronounced way: the R_g curve in the conformation plot is strongly bent in the low molar mass range. The reason for this behaviour is the enlarged sensitivity of the R_g value for high molar mass molecules in the case of co-elution. The curvature of the conformation plot from HT-SEC prevents a correct determination of the branching in the LDPE samples. The lower hydrodynamic volume of branched molecules leads to a reduced slope of the R_g–M relationship which is significantly lower than the value of 0.588 for a linear polymer [204]. Since HT-AF4 shows no co-elution effects the conformation plot provides correct information about the chain branching. The R_g–M_w dependence is linear and the reduced slopes of 0.32 and 0.36 for samples 1 and 2, respectively, indicate very compact macromolecules as a result of the very high degree of branching.

Another interesting feature of HT-AF4 is that the thermo-oxidative degradation of polyolefins in solution can be visualized [203]. This approach can be used to evaluate effects that are caused by improper sample treatment including sample preparation for HT-SEC.

To summarize, the application of AF4 for the characterization of polyolefins allows an extended view of molecular properties which apparently are more complex than has been found by traditional separation methods in the past.

5 Conclusions and Outlook

Polyolefins are one of the most important synthetic polymeric materials in all spheres of human activities ranging from packaging and construction to computer science and medicine. Similar to other polymeric materials, polyolefins are distributed in their molecular properties and in-depth analysis of these properties is required using the most sophisticated analytical methods. This helps to establish structure–property relationships and broadens the application of polyolefins in science and technology. In this review we have discussed recent developments in different analytical techniques for polyolefin analysis.

The classical techniques for chemical composition analysis of polyolefins are based on crystallization behaviour of different components of these materials. These techniques are only applicable for the crystalline part of the sample and the amorphous part is obtained as a bulk fraction. Nevertheless, these techniques are still the analytical workhorse in most polyolefin research laboratories. The reason behind this is that most of the commercially important polyolefin materials are semi-crystalline. There has been a number of recent advances in these techniques that have enabled a reduction in analysis time, better resolution and mathematical modelling etc. The most fascinating innovation in this regard is the development of CEF. CEF combines the separation powers of both TREF and CRYSTAF, resulting in better separation of fractions along with considerable reduction in analysis time. CEF has the promise and potential to be the major technique in crystallization analysis in future.

High-temperature SEC is the premier technique for information regarding molar masses. A number of different concentration detectors as well as molar mass sensitive detectors can be used. The coupling of SEC with spectroscopic techniques like FTIR and ^{1}H-NMR reveals the chemical composition across the MMD of the sample.

A fascinating new development in column based chromatographic techniques for polyolefin analysis is high-temperature interaction chromatography. In contrast to crystallization based techniques, IC can address the whole sample irrespective of whether it is crystalline or amorphous. The use of gradient HT-HPLC, liquid chromatography at critical conditions at high temperatures above 120°C, and HT-HPLC based on precipitation-redissolution or adsorption–desorption for chemical composition analysis of polyolefins have been reported in recent years. These methods are a major breakthrough in the field of chemical composition analysis of polyolefins. They overcome the drawbacks of other techniques used previously for chemical composition analysis as they address both the amorphous and the crystalline part of the sample. The ultimate recent development in polyolefin

analysis is the coupling of HT-HPLC with online SEC. This fascinating development leads to the MMD of the sample as a function of its chemical composition. 2D-HT-HPLC is a major advancement in polyolefin analysis and promises to be the future for research-oriented polyolefin laboratories. The most recent step regarding hyphenation of 2D-HT-HPLC is the coupling with infrared and light scattering detectors [179]. Field flow fractionation overcomes the column-related problems of previous separation techniques like sample degradation or sample loss due to interaction with the stationary phase or the column frits. HT-AF4 is particularly useful for ultrahigh molar mass samples and can emerge as the first choice for very high molar mass polyolefins in future.

To summarize, all techniques used for polyolefin characterization have advantages and disadvantages. Some information can be obtained more reliably from one technique and some other from other techniques. One really has to decide on the problems to be addressed using a given technique. Nevertheless, 2D-HT-HPLC seems to be one major technique to be used for polyolefin analysis in the future due to its ability to provide MMD as a function of CCD of the sample which is not possible by other approaches.

The fact that there is constant progress in developing new separation methods for polyolefins has been demonstrated very recently by the introduction of high-temperature thermal gradient interaction chromatography by Cong et al. In addition to using an interacting stationary phase, temperature gradients are used to enhance separation of complex olefin copolymers.

References

1. Kaminsky W, Arndt M (1997) Polymer synthesis/polymer catalysis. Springer, Berlin, pp 143–187
2. Seymour RB, Cheng T (eds) (1986) History of polyolefins. D. Reidel Publishing Co, Dordrecht
3. Scheirs J, Kaminsky W (2000) Metallocene-based polyolefins: preparation, properties and technology. Wiley, Hoboken
4. Kaminsky W (2008) Macromol Chem Phys 209:459–466
5. Mori S, Barth HG (1999) Size exclusion chromatography. Springer, Berlin
6. Striegel AM, Yau WW, Kirkland JJ, Bly DD (2009) Modern size-exclusion liquid chromatography. Wiley, Hoboken
7. Flory PJ (1953) Principles of polymer chemistry, chaps 12 and 13. Cornell University Press, Ithaca
8. Wunderlich B (1980) Macromolecular physics, vol 3, chaps 8 and 10. Academic, New York
9. Desreux V, Spiegels M (1950) Bull Soc Chim Belg 59:476
10. Shirayama K, Okada T, Kita S (1965) J Polym Sci A 3:907916
11. Wild L (1991) Adv Polym Sci 98:1–47
12. Soares JBP, Hamielec AE (1995) Polymer 36:1639–1654
13. Anantawaraskul S, Soares JBP, Wood-Adams PM (2005) Adv Polym Sci 182:1–54
14. Tomba JP, Carella JM, Pastor JM (2005) J Polym Sci Part B: Polym Phys 43:3083–3092
15. Suzuki S, Nakamura Y, Kamrul Hasan ATM, Liu B, Terano M, Nakatani H (2005) Polym Bull 54:311–319

16. Kissin YV, Mirabella FM, Meverden CC (2005) J Polym Sci Part A: Polym Chem 43:4351–4362
17. Schmidt CU, Busch M, Lilge D, Wulkow M (2005) Macromol Mater Eng 290:404–414
18. Gupta P, Wilkes GL, Sukhadia AM, Krishnaswamy RK, Lamborn MJ, Wharry SM, Tso CC, DesLauriers PJ, Mansfield T, Beyer FL (2005) Polymer 46:8819–8837
19. Kamrul Hasan ATM, Liu B, Terano M (2005) Polym Bull 54:225–236
20. Liu Y, Bo S, Zhu Y, Zhang W (2005) J Appl Polym Sci 97:232–239
21. Xu JT, Jin W, Fu ZS, Fan ZQ (2005) J Appl Polym Sci 98:243–246
22. Zhang Y (2006) J Appl Polym Sci 99:845–851
23. Aust N, Gahleitner M, Reichelt K, Raninger B (2006) Polymer Testing 25:896–903
24. Kissin YV, Chadwick JC, Mingozzi I, Morini G (2006) Macromol Chem Phys 207:1344–1350
25. Assumption HJ, Vermeulen JP, Jarrett WL, Mathias LJ, van Reenen AJ (2006) Polymer 47:67–74
26. Harding GW, van Reenen AJ (2006) Macromol Chem Phys 207:1680–1690
27. Nakatani H, Matsuoka H, Suzuki S, Taniike T, Boping L, Terano M (2007) Macromol Symp 257:112–121
28. Caballero MJ, Suarez I, Coto B, Van Grieken R, Monrabal B (2007) Macromol Symp 257:122–130
29. Shan CLP, Hazlitt LG (2007) Macromol Symp 257:80–93
30. Ortin A, Monrabal B, Sancho-Tello J (2007) Macromol Symp 257:13–28
31. Soares JBP (2007) Macromol Symp 257:1–12
32. Tanase S, Katayama K, Yabunouchi N, Sadashima T, Tomotsu N, Ishihara N (2007) J Mol Catal A: Chem 273:211–217
33. Yau WW (2007) Macromol Symp 257:29–45
34. Nakatani H, Manabe N, Yokota Y, Minami H, Suzuki S, Yamaguchi F, Terano M (2007) Polym Int 56:1152–1158
35. Albrecht A, Brüll R, Macko T, Sinha P, Pasch H (2008) Macromol Chem Phy 209:1909–1919
36. Zhu H, Monrabal B, Han CC, Wang D (2008) Macromolecules 41:826–833
37. Stéphenne V, Bailly C, Berghmans H, Daoust D, Godard P (2008) Polym Int 57:1265–1274
38. Tochácek J, Jancár J, Kalfus J, Zborilová P, Burán Z (2008) Polym Degrad Stab 93:770–775
39. Amer I, van Reenen A (2009) Macromol Symp 282:33–40
40. Anantawaraskul S, Bongsontia W, Soares JBP (2009) Macromol Symp 282:167–174
41. Vadlamudi M, Subramanian G, Shanbhag S, Alamo RG, Varma-Nai M, Fiscus DM, Brown GM, Lu C, Ruff CJ (2009) Macromol Symp 282:1–13
42. Zhang Z (2009) Macromol Symp 282:111–127
43. Sun F, Fu Z, Xu J, Deng Q, Fan Z (2009) Int J Polym Anal Charact 14:437–453
44. Soo Ko Y, Jeon JK, Yim JH, Park YK (2009) Macromol Res 17:296–300
45. de Goede E, Mallon P, Pasch H (2010) Macromol Mater Eng 295:366–373
46. Hasan ATMK, Fang Y, Liu B, Terano M (2010) Polymer 51:3627–3635
47. Kuhlman RL, Klosin J (2010) Macromolecules 43:7903–7904
48. Jørgensen JK, Larsen Å, Helland I (2010) e-polymers 143
49. Harding GW, van Reenen AJ (2011) Eur Polym J 47:70–77
50. Monrabal B (1994) J Appl Polym Sci 52:491–499
51. Soares JBP, Anantawaraskul S (2005) J Polym Sci Part B: Polym Phys 43:1557–1570
52. Gemoets F, Hagen H (2005) Macromol Theory Simul 14:158–163
53. Weiser MS, Mülhaupt R (2006) Macromol Symp 236:111–116
54. Wet-Roos DDE, Toit ADU, Joubert DJ (2006) J Polym Sci Part A: Polym Chem 44:6847–6856
55. Weiser MS, Thomann Y, Heinz LC, Pasch H, Mülhaupt R (2006) Polymer 47:4505–4512
56. Monrabal B, Takeshi Shiono KN, Minoru T (2006) Studies in surface science and catalysis. Elsevier, Amsterdam, pp 35–42

57. Anantawaraskul S, Soares JBP, Jirachaithorn P, Limtrakul J (2006) J Polym Sci Part B: Polym Phys 44:2749–2759
58. Luruli N, Heinz LC, Grumel V, Brüll R, Pasch H, Raubenheimer HG (2006) Polymer 47:56–66
59. Van Grieken R, Carrero A, Suarez I, Paredes B (2007) Macromol Symp 259:243–252
60. Anantawaraskul S, Jirachaithorn P, Soares JBP, Limtrakul J (2007) J Polym Sci Part B: Polym Phys 45:1010–1017
61. Kissin YV, Fruitwala HA (2007) J Appl Polym Sci 106:3872–3883
62. Islam MA, Hussein IA, Atiqullah M (2007) Eur Polym J 43:599–610
63. Anantawaraskul S, Soares JBP, Jirachaithorn P (2007) Macromol Symp 257:94–102
64. Macko T, Schulze U, Brüll R, Albrecht A, Pasch H, Fónagy T, Häussler L, Iván B (2008) Macromol Chem Phys 209:404–409
65. Kissin YV, Brandolini AJ, Garlick JL (2008) J Polym Sci Part A: Polym Chem 46:5315–5329
66. Anantawaraskul S, Somnukguandee P, Soares JBP, Limtrakul J (2009) J Polym Sci Part B: Polym Phys 47:866–876
67. Xia W, Taniike T, Terano M, Fujitani T, Liu B, Soares JBP (2009) Macromol Symp 285:74–80
68. Anantawaraskul S, Somnukguande P, Soares JBP (2009) Macromol Symp 282:205–215
69. Alghyamah AA, Soares JBP (2009) Macromol Rapid Comm 30:384–393
70. Alghyamah AA, Soares JBP (2009) Macromol Symp 285:81–89
71. Anantawaraskul S, Chokputtanawuttilerd N (2009) Macromol Symp 282:150–156
72. Macko T, Bruell R, Brinkmann C, Pasch H (2009) J Autom Meth Manag Chem No. 357026
73. Fischlschweiger M, Aust N, Oberaigner ER, Kock C (2010) Macromol Chem Phys 211:383–392
74. Gao F, Xia X, Mao B (2011) J Appl Polym Sci 120:36–42
75. Monrabal B, del Hierro P (2011) Anal Bioanal Chem 399:1557–1561
76. Monrabal B, Sancho-Tello J, Mayo N, Romero L (2007) Macromol Symp 257:71–79
77. Monrabal B, Romero L, Mayo N, Sancho-Tello J (2009) Macromol Symp 282:14–24
78. Hermel-Davidock T, Cong R, Mehmet D (2010) Polymer Preprints 51:95–96
79. Suriya K, Anantawaraskul S, Soares JBP (2011) J Polym Sci Part B: Polym Phys 49:678–684
80. Pasch H, Trathnigg B (1997) HPLC of polymers. Springer, Berlin
81. Rao B, Balke ST, Mourey TH, Schunk TC (1996) J Chromatogr A 755:27–35
82. Ying Q, Xie P, Liu Y, Qian R (1986) J Liq Chromatogr 9:1233–1243
83. Ibhadon AO (1991) J Appl Polym Sci 42:1887–1890
84. Ying Q, Ye M (1985) Macromol Chem Rapid Comm 6:105–110
85. Parth M, Aust N, Lederer K (2003) Int J Polym Anal Charact 8:175–186
86. Mes EPC, De Jonge H, Klein T, Welz RR, Gillespie DT (2007) J Chromatogr A 1154: 319–330
87. Pasti L, Melucci D, Contado C, Dondi F, Mingozzi I (2002) J Sep Sci 25:691–702
88. Sun T, Brant P, Chance RR, Graessley WW (2001) Macromolecules 34:6812–6820
89. Barth HG, Carlin FJ Jr (1984) J Liq Chromatogr 7:1717–1738
90. Pasch H (2000) Adv Polym Sci 150:1–66
91. Pang S, Rudin A (1992) Polymer 33:1949–1952
92. Wintermantel M, Antonietti M, Schmidt M (1993) J Appl Polym Sci Appl Polym Symp 52:91
93. Degoulet C, Nicolai T, Durand D, Busnel JP (1995) Macromolecules 28:6819–6824
94. Jackson C, Chen YJ, Mays JW (1996) J Appl Polym Sci 61:865–874
95. Yau WW, Arora KS (1994) Polym Mater Sci Eng 69:210
96. Jackson C, Barth HG (1994) Trends Polym Sci 2:203–207
97. Yau WW (1990) Chemtracts-Macromol Chem 1:1–36
98. Hellgeth JW, Taylor LT (1987) Anal Chem 59:295–300
99. Wang CP, Sparks DT, Williams SS, Isenhour TL (1984) Anal Chem 56:1268–1272
100. Johnson CC, Taylor LT (1984) Anal Chem 56:2642–2647
101. Sabo M, Gross J, Wang JS, Rosenberg IE (1985) Anal Chem 57:1822–1826

102. Kok SJ, Wold AS, Hankemeier T, Schoenmakers PJ (2003) J Chromatogr A 1017:83–96
103. Housaki T, Satoh K, Nishikida K, Morimoto M (1988) Makromol Chem Rapid Comm 9:525–528
104. Nishikida K, Housaki T, Morimoto M, Kinoshita T (1990) J Chromatogr A 517:209–217
105. Markovich RP, Hazlitt LG, Smith-Courtney L (1993) Chromatography of polymers. In: Provder T (ed) Characterization by SEC and FFF. ACS Symposium Series, vol 521. American Chemical Society, Washington, DC
106. Dhenin V, Rose LJ (2000) Polymer Preprints 41:285
107. DesLauriers PJ, Battiste DR (1995) ANTEC-SPE 53:3639
108. DesLauriers PJ, Rohlfing DC, Hsieh ET (2002) Polymer 43:159–170
109. DesLauriers PJ (2005) Measuring compositional heterogeneity in polyolefins using SEC/FTIR spectroscopy. In: Striegel A (ed) Multiple detection in size exclusion chromatography. ACS Symposium Series, vol 893. American Chemical Society, Washington, DC
110. Piel C, Albrecht A, Neubauer C, Klampfl CW, Reussner J (2001) Anal Bioanal Chem 400:2607–2613
111. Wheeler LM, Willis JN (1993) Appl Spectrosc 47:1128–1130
112. Willis JN, Dwyer JL, Liu MX (1995) Proc. Int. GPC Symp., Lake Buena Vista, p 345
113. Willis JN, Dwyer JL, Wheeler LM (1993) Polym Mat Sci 69:120–121
114. Polymer Standards Service (Mainz, Germany) webpage: www.polymer.de
115. Pasch H (2001) Macromol Symp 165:91–98
116. Tackx P, Bremmers S (1997) Proc. ISPAC-10, Toronto, 42
117. Albrecht A, Bruell R, Macko T, Malz F, Pasch H (2009) Macromol Chem Phys 210:1319–1330
118. Albrecht A, Bruell R, Macko T, Sinha P, Pasch H (2008) Macromol Chem Phys 209:1909–1919
119. Heinz LC, Graef S, Macko T, Bruell R, Balk S, Keul H, Pasch H (2005) e-polymers 54
120. Macko T, Schulze U, Bruell R, Albrecht A, Pasch H, Fonagy T, Haeussler L, Ivan B (2008) Macromol Chem Phys 209:404–409
121. Verdurmen-Noel L, Baldo L, Bremmers S (2001) Polymer 42:5523–5529
122. de Goede S, Bruell R, Pasch H, Marshall N (2003) Macromol Symp 193:35–44
123. de Goede S, Bruell R, Pasch H, Marshall N (2004) e-polymers 012
124. de Goede E, Mallon P, Pasch H (2010) Macromol Mat Eng 295:366–373
125. de Goede E, Mallon P, Pasch H (2012) Macromol Mat Eng 297:26–38
126. de Goede E, Mallon P, Rode K, Pasch H (2011) Macromol Mat Eng 296:1018–1027
127. Graef S, Bruell R, Pasch H, Wahner UM (2003) e-polymers 005
128. Luruli N, Pipers T, Bruell R, Grumel V, Pasch H, Mathot VBF (2007) J Polym Sci Polym Phys 45:2956–2965
129. Kearney T, Dwyer JL (2008) Am Lab 40:8–9
130. Hiller W, Pasch H, Macko T, Hoffmann M, Ganz J, Spraul M, Braumann U, Streck R, Mason J, Van Damme F (2006) J Magn Res 183:290–302
131. Zhou Z, Kuemmerle R, Stevens JC, Redwine D, He Y, Qiu X, Cong R, Klosin J, Montanez N, Roof G (2009) J Magn Res 200:328–333
132. Zhou Z, Stevens JC, Klosin J, Kuemmerle R, Qiu X, Redwine D, Cong R, Taha A, Winniford B, Chauvel P, Montanez N (2009) Macromolecules 42:2291–2292
133. Cong R, de Groot AW, Parrott A, Yau W, Hazlitt L, Brown R, Miller MD, Zhou Z (2011) Macromolecules 44:3062–3072
134. Berek D (2000) Prog Polym Sci 25:873–908
135. Chang T (2003) Adv Polym Sci 163:1–60
136. Macko T, Pasch H, Kazakevich YV, Fadeev AY (2003) J Chromatogr A 988:69–76
137. Macko T, Pasch H, Denayer JF (2003) J Chromatogr A 1002:55–62
138. Macko T, Bruell R, Pasch H (2003) Chromatographia 57:S39–S43
139. Macko T, Denayer JF, Pasch H, Baron GV (2003) J Sep Sci 26:1569–1574
140. Macko T, Denayer JF, Pasch H, Pan L, Li J, Raphael A (2004) Chromatographia 59:461–467

141. Macko T, Pasch H, Denayer JF (2005) J Sep Sci 28:59–64
142. Wang X, Rusa CC, Hunt MA, Tonelli AE, Macko T, Pasch H (2005) Macromolecules 38:12040
143. Macko T, Bruell R, Zhu Y, Wang Y (2010) J Sep Sci 33:3446–3454
144. Macko T, Bruell R, Brinkmann C, Pasch H (2009) J Autom Meth Manag Chem ID 357026 (electronic journal)
145. Macko T, Pasch H, Bruell R (2006) J Chromatogr A 1115:81–87
146. Macko T, Pasch H, Milonjic SK, Hiller W (2006) Chromatographia 64:183–190
147. Heinz LC, Macko T, Williams A, O'Donohue S, Pasch H (2006) The column (electronic journal), Feb 13–19
148. Macko T, Hunkeler D (2003) Adv Polym Sci 163:61–136
149. Heinz LC, Macko T, Pasch H, Weiser MS, Mülhaupt R (2006) Int J Polym Anal Charact 11:47–55
150. Heinz LC, Graef S, Macko T, Brüll R, Balk S, Keul H, Pasch H (2005) e-polymers 054
151. Lehtinen A, Paukkeri R (1994) Macromol Chem Phys 195:1539–1556
152. Heinz LC, Pasch H (2005) Polymer 46:12040–12045
153. Albrecht A, Heinz LC, Lilge D, Pasch H (2007) Macromol Symp 257:46–55
154. Dolle V, Albrecht A, Brüll R, Macko T (2011) Macromol Chem Phys 212:959–970
155. Albrecht A, Brüll R, Macko T, Pasch H (2007) Macromolecules 40:5545–5551
156. Pasch H, Albrecht A, Bruell R, Macko T, Hiller W (2009) Macromol Symp 282:71–80
157. Gilbert MT, Knox JH, Kaur B (1982) Chromatographia 16:138–146
158. Macko T, Pasch H, Wang Y (2009) Macromol Symp 282:93–100
159. Macko T, Pasch H (2009) Macromolecules 42:6063–6067
160. Macko T, Brüll R, Wang Y (2009) Polym Prepr (Am Chem Soc Div Polym Chem) 50:228–229
161. Macko T, Brüll R, Alamo RG, Stadler FJ, Losio S (2011) Anal Bioanal Chem 399:1547–1556
162. Macko T, Brüll R, Alamo RG, Thomann Y, Grumel V (2009) Polymer 50:5443–5448
163. Macko T, Brüll R, Wang Y, Thomann Y (2009) Column (electronic journal) 4:15–19
164. Macko T, Brüll R, Wang Y, Coto B, Suarez I (2011) J App Polym Sci 122:3211–3217
165. Macko T, Cutillo F, Bussico V, Brüll R (2010) Macromol Symp 298:182–190
166. Chitta R, Macko T, Brüll R, van Doremaele G, Heinz LC (2011) J Polym Sci Part A: Polym Chem 49:1840–1846
167. Ginsburg A, Macko T, Dolle V, Bruell R (2011) Eur Polym J 47:319–329
168. Miller MD, deGroot AW, Lyons JW, Van Damme FA, Winniford BL (2011) J Appl Polym Sci 123:1238–1244
169. Macko T, paper in preparation
170. Lipatov YS, Sergeeva LM (1974) Adsorption of polymers. Wiley, New York
171. Lochmüller CH, Moebus MA, Liu QC, Jung C, Elomaa M (1996) J Chromatogr Sci 34:69–76
172. Lee HC, Chang T (1996) Polymer 37:S747–S749
173. Pasch H (2004) Characterization of polymer heterogeneity by 2D-LC. In: Striegel AM (ed) multiple detection in size-exclusion chromatography. ACS Symposium Series, vol 893. American Chemical Society, Washington, DC
174. Rittig F, Pasch H (2008) Multidimensional liquid chromatography in industrial applications. In: Cohen S, Schure M (eds) Multidimensional liquid chromatography: theory and applications in industrial chemistry and life sciences. Wiley, New York
175. Raust JA, Houillot L, Charleux B, Moire C, Farcet C, Pasch H (2010) Macromolecules 43:8755–8765
176. Mass V, Bellas V, Pasch H (2008) Macromol Chem Phys 209:2026–2039
177. Ginsburg A, Macko T, Dolle V, Bruell R (2010) J Chromatogr A 1217:6867–6874
178. Roy A, Miller MD, Meunier DM, de Groot AW, Winniford WL, van Damme FA, Pell RJ, Lyons JW (2010) Macromolecules 43:3710–3720
179. Lee D, Miller MD, Meunier DM, Lyons JW, Bonner JM, Pell RJ, Li Pi Chan C, Huang T (2011) J Chromatogr A 1218:7173–7179

180. Myers MN (1997) J Microcolumn Sep 9:151–162
181. Giddings JC (1993) Science 260:1456–1466
182. Williams SKR, Lee D (2006) J Sep Sci 29:1720–1732
183. Williams SKR, Benincasa MA (2000) Field-flow fractionation analysis of polymers and rubbers. In: Meyers RA (ed) Encyclopedia of analytical chemistry: instrumentation and applications. Wiley, Chichester, pp 7582–7608
184. Lee D, Williams SKR (2005) Proc. 56th Pittsburgh conference on analytical chemistry and applied spectroscopy
185. Schimpf ME, Caldwell KD, Giddings JC (eds) (2000) Field-flow fractionation handbook. Wiley, New York
186. Janca J (1988) Field-flow fractionation: analysis of macromolecules and particles. In: Chromatographic science series, vol 39. Marcel Dekker, NY
187. Benincasa MA, Giddings JC (1997) J Microcolumn Sep 9:479–495
188. Podzimek S (2011) Light scattering, size exclusion chromatography and asymmetric flow field flow fractionation. Wiley, Hoboken
189. Lee H, Williams SKR, Wahl KL, Valentine NB (2003) Anal Chem 75:2746–2752
190. Giddings JC (1966) Sep Sci 1:123–125
191. Caldwell KD, Kesner LF, Myers MN, Giddings JC (1972) Science 176:296–298
192. Liu G, Giddings JC (1992) Chromatographia 3:483–492
193. Wahlund KG, Giddings JC (1987) Anal Chem 59:1332–1339
194. Kirkland JJ, Yau WW, Szoka FC (1982) Science 215:296–298
195. Giddings JC, Myers NM, Caldwell KD (1981) J Sep Sci Tech 16:549–575
196. Messaud FA, Sanderson RD, Runyon JR, Otte T, Pasch H, Ratanathanawongs Williams SK (2009) Prog Polym Sci 34:351–368
197. Miller ME, Giddings JC (1998) J Micro Sep 10:75–78
198. Gao S, Caldwell D, Myers N, Giddings JC (1985) Macromolecules 18:1272–1277
199. Otte T, Macko T, Brüll R, Pasch H (2009) Polymer Preprints 50(2):727
200. Otte T, Brüll R, Macko T, Klein T, Pasch H (2010) J Chromatogr A 1217:722–730
201. Otte T, Pasch H, Macko T, Brüll R, Stadler FJ, Kaschta J, Becker F, Buback M (2011) J Chromatogr A 1218:4257–4267
202. Otte T, Klein T, Brüll R, Macko T, Pasch H (2011) J Chromatogr A 1218:4240–4248
203. Otte T, Pasch H, Brüll R, Macko T (2011) Macromol Chem Phys 212:401–410
204. Le Guillou JC, Zinn-Justin J (1977) Phys Rev Lett 39:95–98

http://www.springer.com/978-3-642-34329-2

Polymer Composites - Polyolefin Fractionation - Polymeric Peptidomimetics - Collagens

Abe, A.; Kausch, H.-H.; Möller, M.; Pasch, H. (Eds.)

2013, VI, 210 p., Hardcover
ISBN: 978-3-642-34329-2